

Constraints on the Age and Provenance of the Chugach Accretionary Complex from Detrital Zircons in the Sitka Graywacke near Sitka, Alaska

By Peter J. Haeussler, George E. Gehrels¹, and Susan M. Karl

Abstract

The Sitka Graywacke is the westernmost and youngest unit of the Chugach accretionary complex in southeastern Alaska. Using laser-ablation inductively coupled plasma mass spectroscopy, we obtained 492 detrital-zircon ages on seven typical samples of Sitka Graywacke turbidites, which were collected in a transect across much of the unit near Sitka, Alaska. Individual grains range in age from 66 to 1,802 m.y. The youngest peak ages on relative-probability plots of the western four samples (74, 72, 74, and 74 m.y., from west to east) are distinctly younger than the youngest peak ages of the eastern three samples (105, 103, and 97 m.y., from west to east). These youngest peak ages set maximum depositional ages for each sample. We suggest that these peak ages are not significantly older (within ~5 m.y.) than the depositional age of the Sitka Graywacke because the deposits accumulated in a trench along a convergent margin, where magmatic sources likely continuously introduced juvenile zircons. The differences in the youngest cluster of detrital-zircon ages between the eastern and western sample localities is likely due to both a change in provenance and a fault. The similarity of the youngest peak ages in the Sitka Graywacke to fossil ages in the Valdez Group, in Prince William Sound, implies that the western part of the Sitka Graywacke is correlative with the Valdez Group, as previously inferred. However, the eastern part of the Sitka Graywacke has youngest detrital-zircon ages older than fossil ages in the Valdez Group and younger than fossil ages in the McHugh Complex, which in south-central Alaska is the oldest part of the accretionary complex. The age distribution of zircons in the older, eastern sequence suggests sources along the British Columbia margin. The detrital-zircon ages in the younger, western sequence are similar to igneous ages from south-central Alaska to southern British Columbia. Right-lateral strike slip on various fault systems inboard of the Sitka Graywacke implies that it lay to the south when it was deposited and offscraped. Thus, although source areas as far north as the St. Elias Mountains and south-central Alaska are possible, they were most likely in coastal and interior British Columbia.

Introduction

Graywacke turbidites are notoriously poor in fossils, and so dating turbidite sequences can be a great challenge. The Sitka Graywacke, which lies along the west coast of southeastern Alaska, is one such turbidite sequence (Berg and Hinckley, 1963; Loney and others, 1963; Decker and others, 1979; Decker, 1980). The unit is part of a Mesozoic through early Tertiary accretionary complex rimming southern Alaska (fig. 1; Plafker and others, 1977) that is commonly referred to as the Chugach terrane (for example, Plafker and others, 1994). Various workers (Nilsen and Moore, 1979; Nilsen and Zuffa, 1982; Plafker and others, 1994) have proposed that these accretionary-complex turbidites were deposited by northward-flowing trench-parallel turbidity currents derived from erosion of the Coast Mountains of southeastern Alaska and British Columbia.

Regional correlations between the Sitka Graywacke and other units of the Chugach accretionary complex are hindered by the absence of fossils in the turbidites. Thus far, only two fossils have been identified from the Sitka Graywacke. Reifenstuhl (1986) obtained a gastropod with a nondiagnostic age ranging from Silurian to Eocene. Also, a small limestone pod, with sharp contacts, in graywacke (at the location of our sample 65, fig. 2) contained a poorly preserved cone-shaped nassellarian radiolarian of possible Jurassic age (C.D. Blome, written commun., 1994).

Detrital-zircon ages can provide a maximum depositional age because the host sediment must have been laid down after the youngest detrital-zircon grain crystallized. In this study, we use the youngest ages from sandstone of the Sitka Graywacke to constrain depositional ages, subdivide the unit, and interpret the provenance of the detrital-zircon grains on the basis of a comparison with the ages of potential igneous source rocks along the northern Cordilleran margin.

Methods

We collected seven samples in an east-west-trending transect across much of the Sitka Graywacke near Sitka, Alaska (fig. 2; table 1). All samples were collected from normally

¹Department of Geosciences, University of Arizona, Tucson.

2 Constraints on the Age and Provenance of the Chugach Accretionary Complex, Alaska

graded sandy turbidite beds, 5 to 20 cm thick, with sharp basal contacts. The sampled beds were typical of the beds at each sample locality. Detrital zircons were extracted by using standard mineral-separation techniques.

Zircons were mounted in epoxy and polished to expose the interior of the grains. Isotopic analyses were performed by using a Micromass IsoProbe multicollector inductively coupled plasma mass spectrometer (MC-ICPMS) with a laser-ablation system at the geochronology laboratory of the University of Arizona, Tucson. Laser-beam diameter was 35 μm , yielding ablation pits \sim 15 μm deep. Interelement fractionation was monitored by analyzing fragments of a large concordant zircon with a known (isotope-dilution thermal-ionization mass-spectrographic, or ID-TIMS) age of 564 ± 4 m.y. (2σ error). This standard was analyzed once for every five unknowns. Grains were selected randomly from all sizes and morphologies present, avoiding grains with fractures or inclusions. The ablated material was carried in Ar gas into the plasma source of the mass spectrometer, which was equipped with a flight tube of sufficient width that U, Th, and Pb isotopes were analyzed simultaneously. All measurements were made in static mode, using Faraday detectors for ^{238}U , ^{232}Th , and 208 – ^{206}Pb and an ion-counting channel for ^{204}Pb . Ion yields were 0.5 mV/ppm. Each analysis consisted of 1 20-s integration on peaks with the laser off (for backgrounds), 20 1-s

integrations with the laser firing, and a 30-s delay to purge the previous sample and prepare for the next analysis.

Common Pb correction was made by using the measured ^{204}Pb content and assuming an initial Pb composition from Stacey and Kramers (1975) (with uncertainties of ± 1.0 for $^{206}\text{Pb}/^{204}\text{Pb}$ ratio and ± 0.3 for $^{207}\text{Pb}/^{204}\text{Pb}$ ratio). Our ^{204}Pb measurement is unaffected by the presence of ^{204}Hg because backgrounds are measured on peaks (thereby subtracting any background ^{204}Hg and ^{204}Pb) and only trace Hg was present in the Ar gas.

Interelement fractionation of Pb/U is generally <20 percent, whereas fractionation of Pb isotopes is generally <5 percent. In-run analysis, generally every fifth measurement, of fragments of a large zircon crystal standard (Sri Lanka) with a known age of 564 ± 4 m.y. (2σ error; G.E. Gehrels, unpub. data, 2004) was used to correct for this fractionation. The uncertainty resulting from the calibration correction (together with the uncertainty from decay constants and common Pb composition) is generally ± 3 percent (2σ) for $^{206}\text{Pb}/^{238}\text{U}$ ages and for $^{206}\text{Pb}/^{207}\text{Pb}$ ages >1.2 b.y. Fractionation also increases with depth into the laser pit. The accepted isotopic ratios were accordingly determined by least-squares projection through the measured values back to the initial determination. The complete measured isotopic ratios and ages are listed in table 2. Errors from measuring $^{206}\text{Pb}/^{238}\text{U}$, $^{206}\text{Pb}/^{207}\text{Pb}$, and $^{206}\text{Pb}/^{204}\text{Pb}$

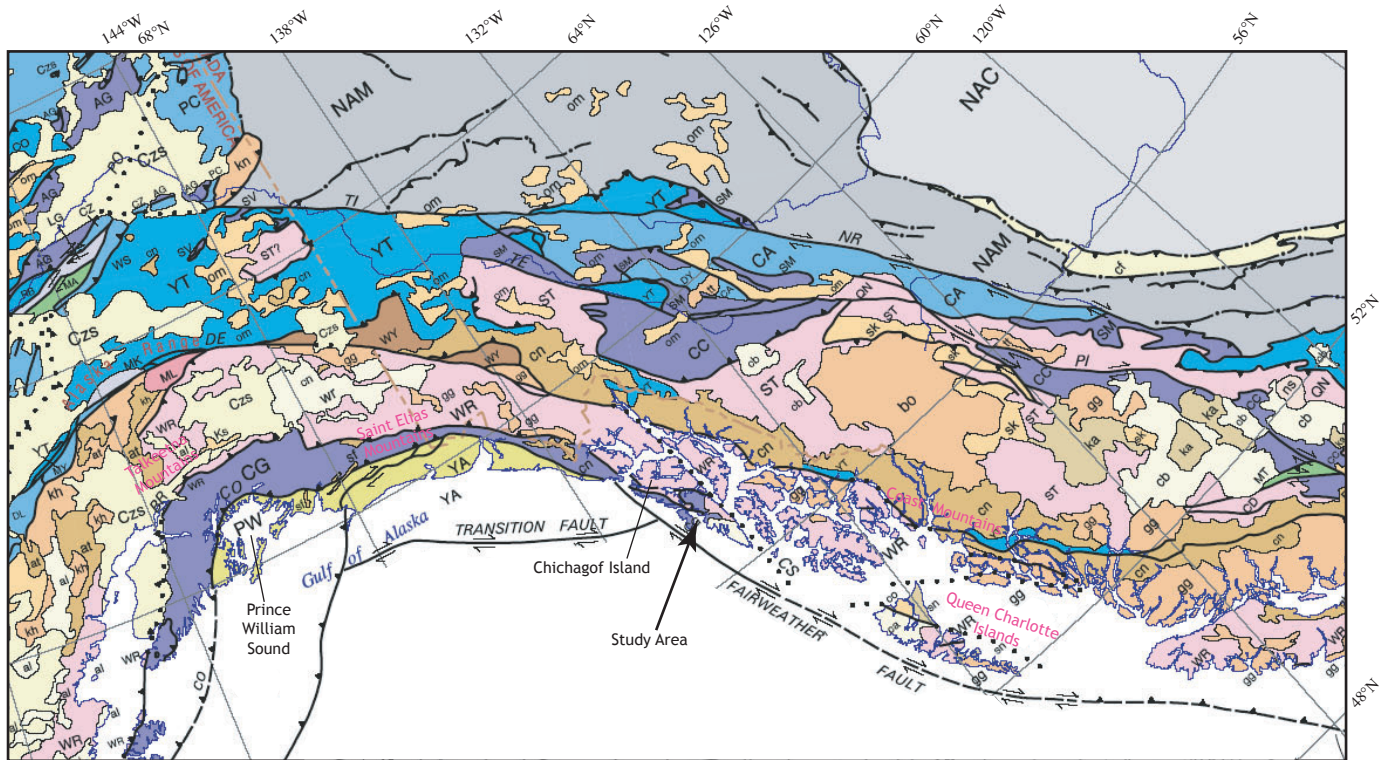


Figure 1. Gulf of Alaska area, showing location of study area and tectonostratigraphic terranes of Alaska, Yukon Territory, and British Columbia (from Nokleberg and others, 1998). The Sitka Graywacke, the Valdez Group, and the McHugh Complex are all parts of the Chugach accretionary complex. Terranes: CG, Chugach; ST, Stikine; YT, Yukon-Tanana. Faults: BR, Border Ranges; CS, Chatham Straight; DE, Denali; TI, Tintina.

Table 1. Summary data for samples of Sitka Graywacke sandstone analyzed for detrital zircons

[Latitude and longitude from NAD27 datum; youngest detrital-zircon age peaks from relative-probability plots in figure 3. USGS, U.S. Geological Survey]

Sample	Field No.	USGS map sheet	Latitude(° N.)	Longitude(° W.)	Youngest detrital-zircon age peak (Ma)
62	92PH062	Port Alexander D-5	56.93681	135.43308	74
63	92PH063	Port Alexander D-5	56.95279	135.39284	72
64	92PH064	Port Alexander D-5	56.97973	135.37554	74
65	92PH065	Port Alexander D-4	56.99984	135.32176	74
66	92PH066	Sitka A-4	57.01497	135.27063	105
67	92PH067	Sitka A-4	57.03072	135.23172	103
69	92PH069	Port Alexander D-4	56.99345	135.15739	97

ratios are reported at the 1σ level. Additional errors that affect all ages include uncertainties from (1) U decay constants, (2) the composition of common Pb (assumed to be ± 1.0 for the $^{206}\text{Pb}/^{204}\text{Pb}$ ratio and ± 0.3 for the $^{207}\text{Pb}/^{204}\text{Pb}$ ratio), and (3) calibration correction. These systematic errors add an additional 2-percent (1σ) uncertainty to $^{206}\text{Pb}/^{238}\text{U}$ ages and to $^{206}\text{Pb}/^{207}\text{Pb}$ ages >1.2 b.y. A total of 69 to 75 ages were determined for each of the seven samples.

Age interpretations for the analyses are based largely on $^{206}\text{Pb}/^{238}\text{U}$ ages. $^{206}\text{Pb}/^{207}\text{Pb}$ ages for these relatively young zircons are much less reliable given the low ^{207}Pb content. As a result, discordance on an individual-grain basis cannot be assessed for grains younger than 1.2 b.y. Thus, $^{206}\text{Pb}/^{207}\text{Pb}$ ages were used for a total of four grains older than 1.2 b.y.

The U-Pb ages are plotted as histograms with a normalized relative-probability distribution in figure 3 (Ludwig, 2003), where the relative height of peaks corresponds to the significance of that age population.

Results and Discussion

We interpret the youngest cluster of detrital-zircon ages as setting a limiting depositional age for that sample. The youngest cluster is used, rather than the youngest individual grain, because isotopic disturbance by Pb loss can yield detrital-zircon ages that are significantly younger than the crystallization age but still analytically concordant. Because each zircon in a group of grains would almost certainly not lose exactly enough Pb to yield similar ages, we interpret the peak age of the youngest cluster (determined from the relative-probability plots in fig. 3) as a robust indicator of the age of the youngest igneous source, accordingly setting a maximum depositional age for the host graywacke.

The detrital-zircon ages indicate that the possible Jurassic nassellarian from the outcrop at sample locality 65, mentioned previously, is likely younger than Jurassic. The youngest peak

in ages at this locality is much younger—74 m.y. This detrital-zircon age helps constrain the loose fossil age.

The youngest peak ages of the western four samples (74, 72, 74, and 74 m.y., from west to east) are distinctly younger

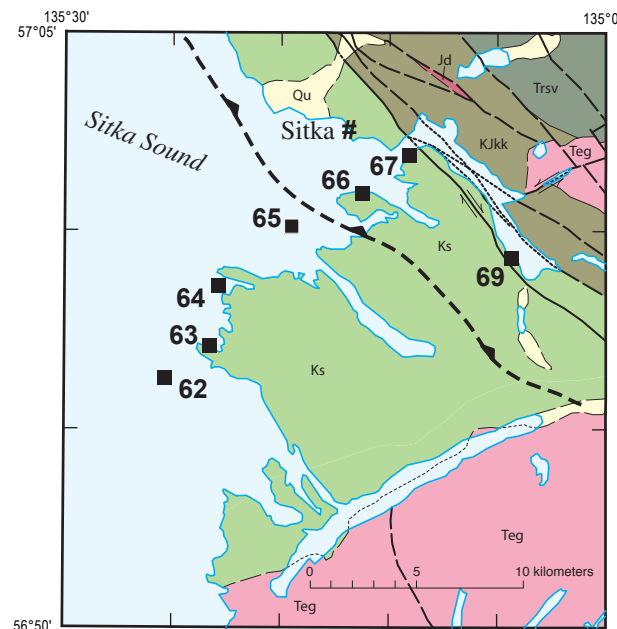


Figure 2. Study area near Sitka, Alaska, showing regional geology simplified from Karl and others (in press). Squares, location of detrital zircon samples. Samples 62 and 65 are on small islands hidden beneath symbol. Irregular dashed line, inferred thrust fault (teeth on upper plate) between samples 65 and 66 that separates older, eastern samples from younger, western samples. Units: Jd, Jurassic diorite; Kjkk and Trsv, Jurassic through Cretaceous and Triassic parts of the Kelp Bay Group, respectively; Ks, Cretaceous Sitka Graywacke; Qu, Quaternary sedimentary rocks, undivided; Teg, Eocene granitic rocks. From U.S. Geological Survey Sitka A-4 and Port Alexander D-5 1:63,360-scale maps.

4 Constraints on the Age and Provenance of the Chugach Accretionary Complex, Alaska

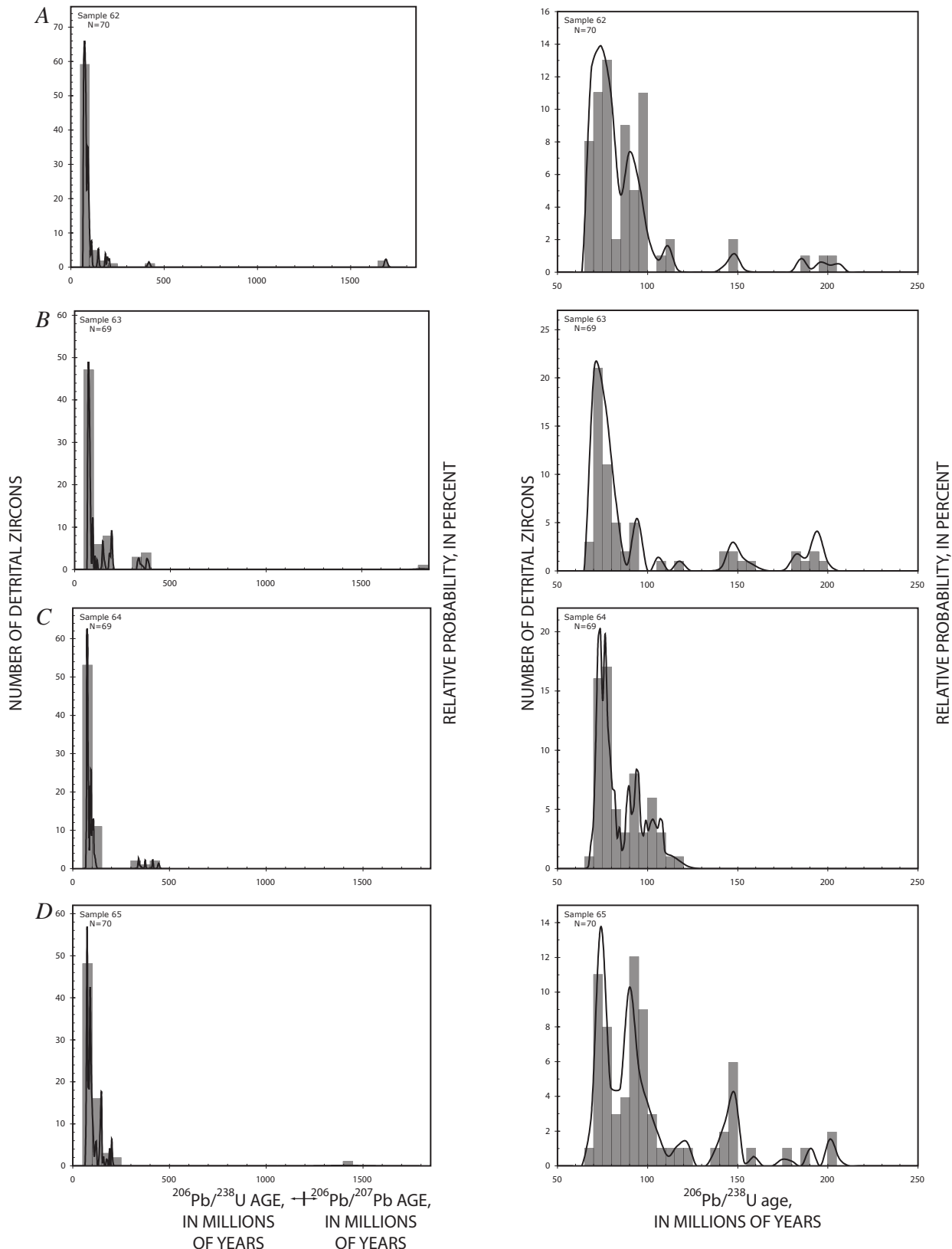


Figure 3. Detrital-zircon histograms (gray bars) and relative-probability plots (solid curve) for samples 62 (A), 63 (B), 64 (C), 65 (D), 66 (E), 67 (F), and 69 (G). Left plot shows complete age range from 0 to 1,850 m.y., with a 50-m.y. bar width; right plot shows detailed area from 50 to 250 m.y., with a 5-m.y. bar width. All plots calculated with Isoplot software (Ludwig, 2003).

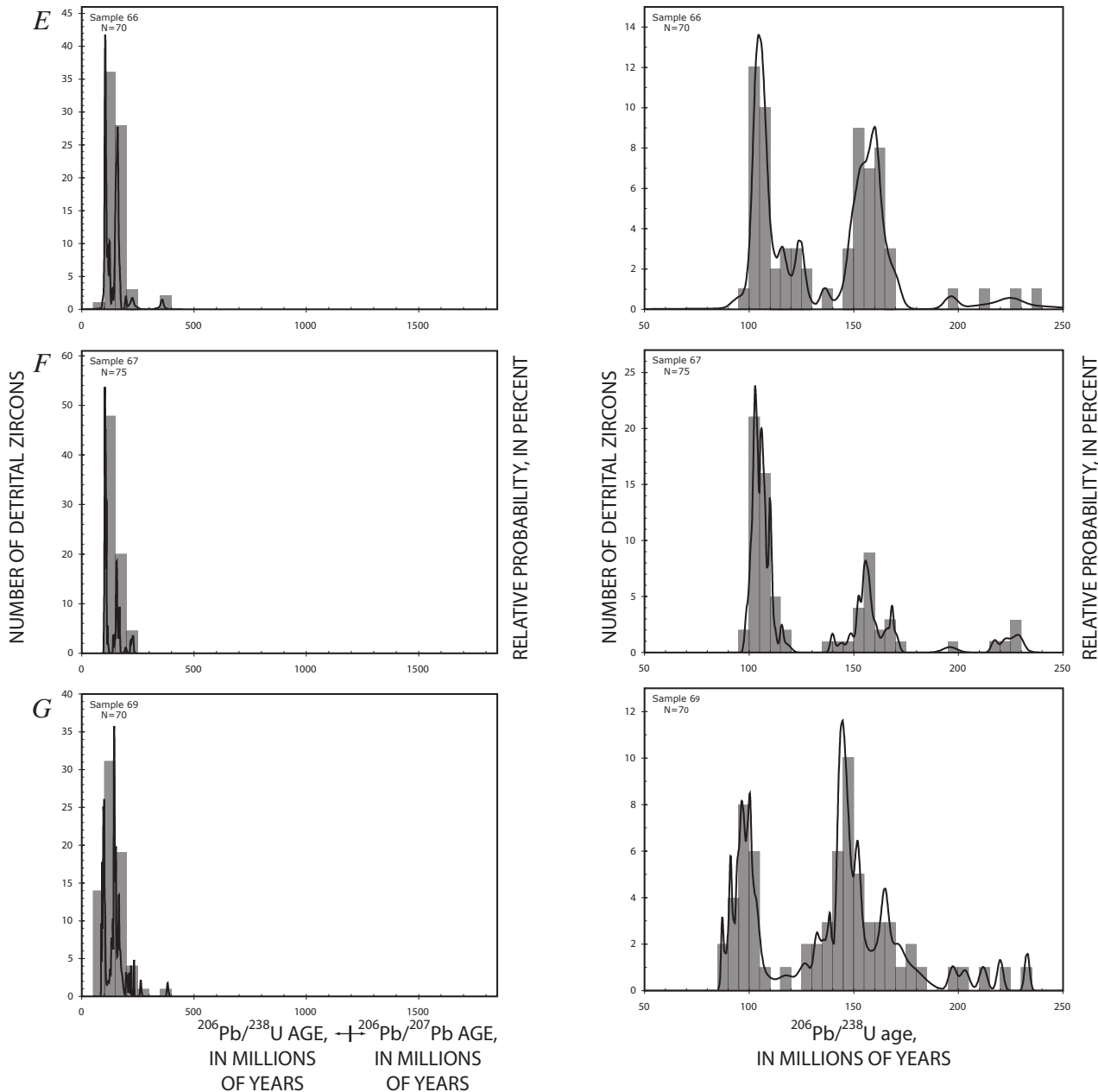


Figure 3.—Continued.

than the youngest peak ages of the eastern three samples (105, 103, and 97 m.y., from west to east; figs. 2, 3; tables 1, 2). Interpretation of these limiting ages depends on the time interval between crystallization and deposition of the zircons, which would largely be influenced by the presence or absence of igneous sources, the rate of exhumation of source terrains, and the geometry and efficiency of depositional systems.

We suggest that the youngest peak ages are close to the depositional age of the Sitka Graywacke. A subduction zone with associated arc magmatism was active along the western margin of North America during Late Cretaceous through early Tertiary time (for example, Miller, 1994; Moll-Stalcup and others, 1994; Plafker and others, 1994; Breitsprecher and Mortensen, 2004a, b), and so numerous sources of juvenile

zircons were present. Also occurring at that time was rapid uplift of the Coast Mountains of southeastern Alaska and British Columbia (for example, Hollister, 1982; Crawford and others, 2000; McClelland and Mattinson, 2000), which would have provided additional sources of young zircons. Moreover, because the Chugach terrane turbidites are considered to have been deposited by northward-flowing currents in the paleotrench (Nilsen and Moore, 1979; Nilsen and Zuffa, 1982; Plafker and others, 1994), little time intervened between deposition and accretion of the trench sediment. Taking these considerations together, we infer little time, possibly ≤ 5 m.y., between crystallization and deposition of the detrital zircons. Thus, these detrital-zircon limiting ages would indicate a range in the maximum age of these Sitka Graywacke samples from ~ 72 to ~ 105 m.y.

6 Constraints on the Age and Provenance of the Chugach Accretionary Complex, Alaska

The difference in the youngest peak ages between the eastern three and western four sample localities may be due to both a change in provenance and a fault. Histograms and relative-probability plots of detrital-zircon ages from the eastern and western samples differ (fig. 3), and so the two population groups are here considered separately. Because the two groups appear to be internally similar, we combined the data for the western four and eastern three samples (fig. 4). Because the patterns of the combined histograms and relative-probability plots differ for the two groups, the provenance must have changed. Is the difference between the two areas due only to a change in provenance? If so, then the entire sampling area would consist of a single stratigraphic section more than 15 km thick. Such a great thickness of a single panel in an accretionary complex would be extremely unusual. The overall westward-younging pattern of the youngest detrital-zircon ages is consistent with the standard model of accretionary prisms, which has trenchward-younging, fault-bounded panels of accreted sediment. Moreover, intraformational thrust faults are nearly ubiquitous in Chugach terrane turbidites (for example, Sample and Moore, 1987). Numerous faults occur within the

Sitka Graywacke, most of which bound thrust panels and others of which are later-stage right-lateral strike-slip faults (Davis and others, 1998; Karl and others, in press). No previous fault was mapped between the western and eastern localities, and no obvious sedimentologic differences exist. We infer a fault, probably a thrust fault, in an uncertain location between the eastern three and western four sample localities (fig. 2).

The detrital-zircon limiting ages for the Sitka Graywacke allow comparison and correlation to other parts of the Chugach accretionary complex in southern Alaska. The Valdez Group comprises the largest area of the Chugach terrane in south-central Alaska (fig. 1). The western four samples of Sitka Graywacke have youngest peak ages of late Campanian (fig. 6) on the time scale of Gradstein and others (2005). Assuming that the detrital zircons were deposited within several million years of crystallization, they indicate that the western part of the Sitka Graywacke is correlative with the Valdez Group (fig. 6; Grant and Higgins, 1910; Tysdal and Plafker, 1978). All reliable fossil ages from the Valdez Group are Maastrichtian (65.5–70.6 m.y.; Tysdal and Plafker, 1978; Nelson and others, 1985), although two samples have questionable age calls

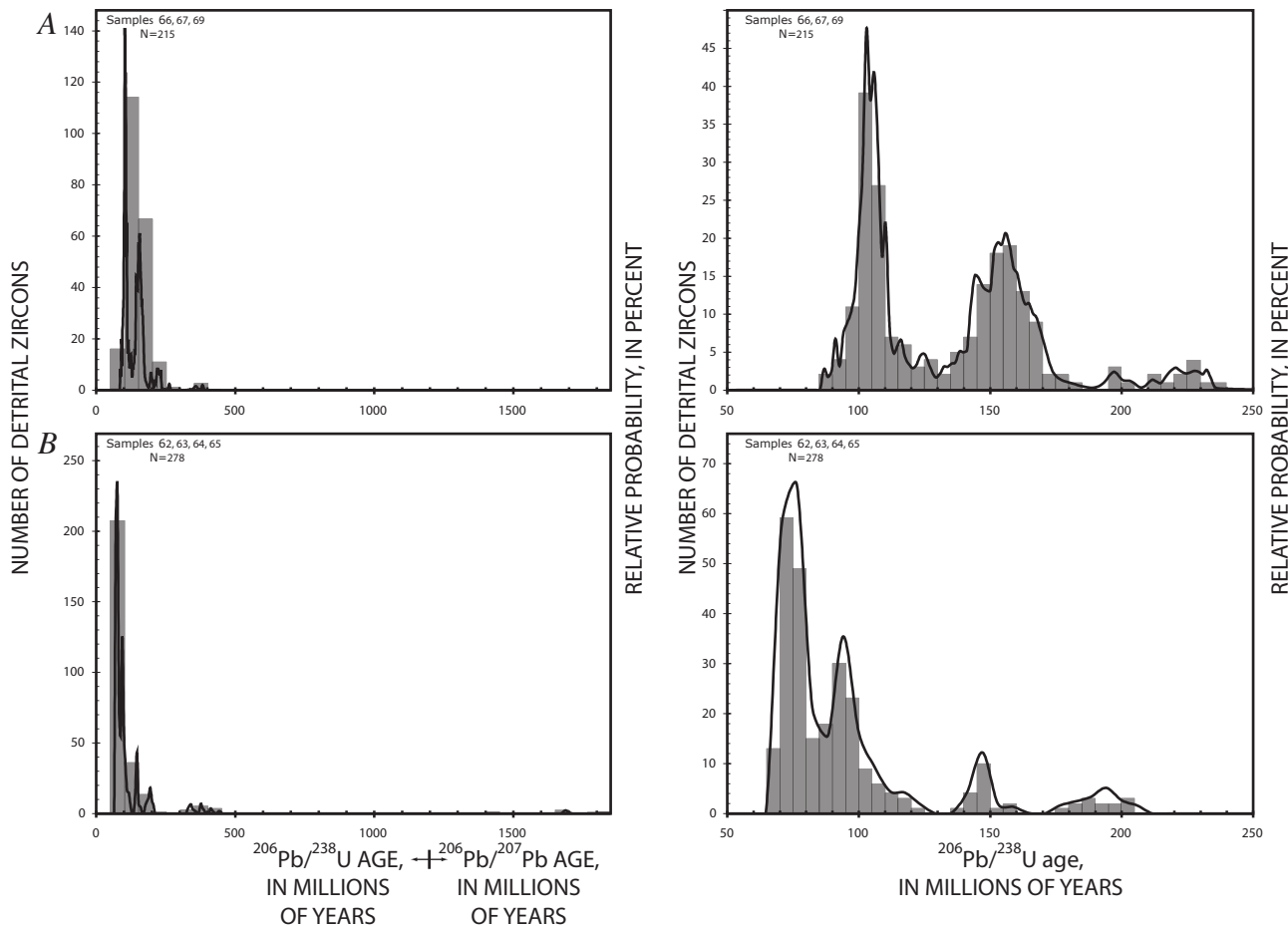


Figure 4. Detrital-zircon histograms and relative-probability plots for eastern three samples (66, 67, 69) (A) and western four samples (62, 63, 64, 65) (B). Same symbols as in figure 3.

that are Campanian-Maastrichtian (65.5–83.5 m.y.; Tysdal and Plafker, 1978; Winkler, 1992). If less than 5 m.y. intervened between crystallization and deposition of the western Sitka Graywacke samples, they would be Maastrichtian.

The younger part of the Sitka Graywacke also appears to be correlative with the upper part of the Yakutat Group of Tarr and Butler (1909). The Yakutat Group consists broadly of an eastern, or “lower,” melange facies and a western, or “upper,” flysch facies, both of which are considered correlative with the Chugach terrane (Plafker and others, 1977, 1994). The Yakutat Group is in the eastern part of the Yakutat terrane (fig. 1), which is presently accreting onto the southern Alaska margin (Plafker and others, 1978, 1994). The Yakutat terrane likely lay south of the Sitka Graywacke, off the coast of southern British Columbia, when it was offscraped (Plafker and others, 1994). Thus, on a large scale, the Yakutat Group was the now-dismembered part of the accretionary complex that lay to the south of the Sitka Graywacke. One Campanian fossil was obtained in outcrop from the upper part of the Yakutat Group (Jones and Clark, 1973), and Campanian and Maastrichtian foraminifers were recovered from an offshore borehole that penetrated the Yakutat Group (W.V. Sliter, in Rau and others, 1983). Flysch of the upper part of the Yakutat Group is more quartzofeldspathic and has a higher proportion of plutonic-rock fragments relative to the Sitka Graywacke and the Valdez Group (Nilsen, 1984). Nonetheless, the similarity of the youngest peak ages for the western four samples of Sitka Graywacke to the fossil ages for the Yakutat Group indicate that the rocks are approximately coeval, as previously considered (for example, Plafker and others, 1994), although they differ compositionally.

The Sitka Graywacke is at least ~30 m.y. older than the older part of the Chugach accretionary complex in southeastern Alaska (fig. 6). The Kelp Bay Group of Berg and Hinkley (1963), a melange containing fossils as young as Valanginian (Plafker and others, 1976; Decker, 1980), lies in fault contact with the Sitka Graywacke (see units KJkk and Trsv, fig. 2). The oldest detrital-zircon limiting age for the Sitka Graywacke is 105 m.y. (sample 66), and so a substantial age gap of ~30 m.y. exists on the time scale of Gradstein and others (2005). Of course, this age gap may be smaller if younger fossils are present in the Kelp Bay Group, or if older samples are present in the Sitka Graywacke.

The youngest peak ages for the eastern three samples of Sitka Graywacke (fig. 2) corresponds to the youngest fossil ages for melange of the McHugh Complex in south-central Alaska (fig. 6; see Plafker and others, 1994, for an overview of ages), which are Albian (99.6–112.0 m.y.) or Cenomanian (99.6–93.5 m.y.; Winkler and others, 1980). The McHugh Complex has been correlated with the Kelp Bay Group (Plafker and others, 1977, 1994; Decker, 1980). The oldest two samples of Sitka Graywacke are Albian (99.6–112.0 m.y.), and the easternmost sample (69) is Cenomanian (93.5–99.6 m.y.). Radiolarians from one small stratigraphically and structurally enigmatic area in Prince William Sound are dated at Coniacian through Turonian (89.3–83.5 m.y.; Haeussler and Nelson, 1993; Nelson and others, 1999), between the ages of the

Valdez Group and the McHugh Complex. Thus, assuming that the detrital-zircon limiting ages are close to the depositional age of the Sitka Graywacke, the age range of the unit is at least ~26–32 m.y.², significantly longer than the age range of reliably dated turbidites of the Valdez Group. Considering all these turbidite sequences together suggests relatively continuous turbidite sedimentation between Albian and Maastrichtian time; however, the volume of sediment deposited varies, and clearly a large pulse was deposited in Maastrichtian time (for example, Plafker and others, 1994).

The distribution of detrital-zircon ages for the Sitka Graywacke corresponds to that of magmatic ages from south-central Alaska to British Columbia. The eastern three samples contain the largest number of zircons dated at 100–110 m.y. (particularly samples 66 and 67) and at 145–165 m.y. (figs. 3, 4). Histograms derived from a compilation of igneous-rock ages from British Columbia (Breitsprecher and Mortenson, 2004a) and Yukon Territory (Breitsprecher and Mortenson, 2004b) are shown in figure 5. Numerous plutons in the Coast Mountains of British Columbia and southeastern Alaska dated at 90–110 m.y. may be the source of these zircons. In south-central Alaska, little magmatism has been reported. Numerous sources are possible, both near and far, for the older ages of 145–165 m.y. that may reflect (1) the Stikine terrane magmatic arc, which lies to the east and south of the study area (fig. 2; Van der Heyden, 1992); (2) plutons on the outer Queen Charlotte Islands in British Columbia (Butler and others, in press), (3) Middle to Late Jurassic plutons in southern British Columbia (for example, van der Heyden, 1992); (4) intrusions in the Saint Elias Mountains (Dodds and Campbell, 1988); or (5) younger phases of the Talkeetna and Chitina plutonic arcs in south-central Alaska (Plafker and others, 1989; Roeske and others, 2003; Trop and others, 2005). These detrital-zircon ages do not uniquely define the source terrain.

The western four samples have ages that are consistent with igneous sources from south-central Alaska to southern British Columbia. All four samples contain zircons dated at ~74 m.y. Plutons at the lower end of this age range occur in the western Alaska Range. Voluminous volcanism occurred in the Talkeetna Mountains of south-central Alaska between 80 and 70 m.y. Detrital zircons from the Cretaceous Matanuska Formation of south-central Alaska have a significant peak in ages of 75–80 m.y. (J.M. Trop, written commun., 2005). Numerous intrusions dated at 57–71 m.y. occur in the region between Juneau and Haines (Gehrels, 2000). A significant peak in detrital-zircon ages from 90–100 m.y. corresponds to a period of voluminous magmatism in southeastern Alaska and British Columbia (fig. 5), and so this peak age seems to reflect

²The younger age comes from 100 m.y. (the youngest peak age for the eastern three samples, at loc. 69) minus 74 m.y. (the oldest peak age for the western four samples, at locs. 62, 64, and 65) equals 26 m.y., whereas the older age comes from 104 m.y. (the oldest peak age for the eastern three samples, at loc. 66) minus 72 m.y. (the youngest peak age for the western four samples, at loc. 63) equals 32 m.y.

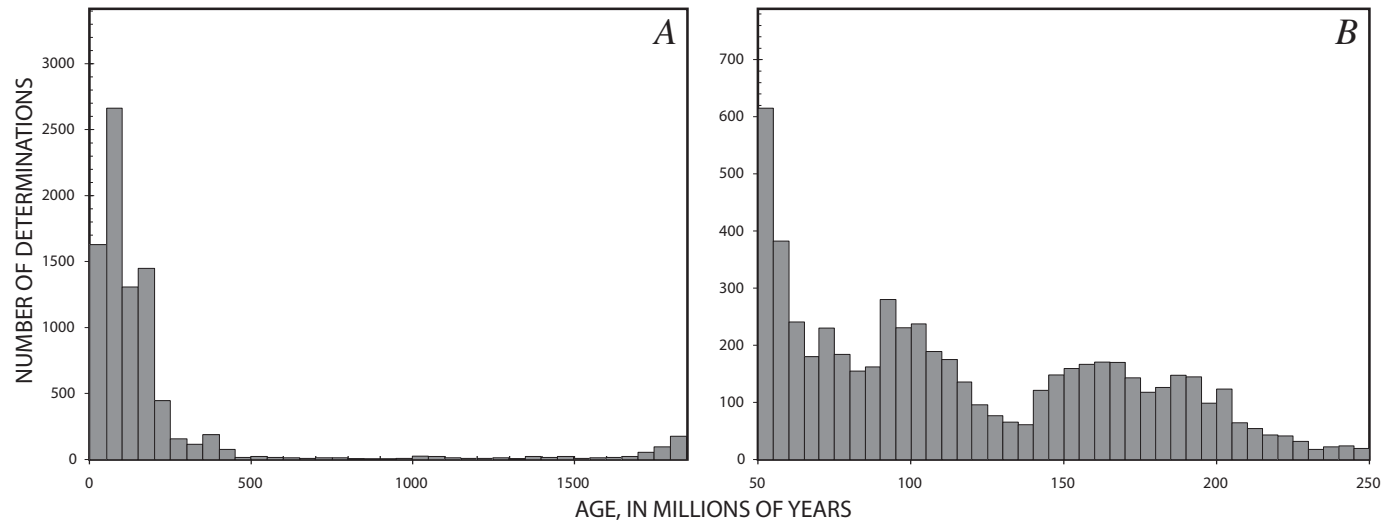


Figure 5. Histograms of 9,318 isotopic-age determinations from British Columbia and Yukon Territory, from compilations by Breitsprecher and Mortensen (2004a, b). *A*, All data. *B*, Data from 50 to 250 m.y., with a 5-m.y. bar width as in figures 3 and 4.

indeterminate sources from this region. Moreover, the relatively small number of zircons dated at 80–90 m.y. is also consistent with the absence of plutons in that interval in southern southeastern Alaska and British Columbia. Interestingly, the only >1-b.y. zircons were obtained from the western, young group of samples: $1,686 \pm 6$, $1,693 \pm 8$, $1,813 \pm 32$, and $1,407 \pm 96$ m.y. ($^{206}\text{Pb}/^{207}\text{Pb}$ ages). These old ages may reflect sources in the northern Cordilleran miogeocline (Gehrels, 2000) or in the Yukon-Tanana terrane of southeastern Alaska and British Columbia (Kapp and Gehrels, 1998; Gehrels, 2001).

In conclusion, the detrital zircons in the samples of Sitka Graywacke do not uniquely identify a source region. Instead, possible source regions cover a vast area from south-central Alaska to southern British Columbia. However, all considerations of the regional tectonics of southeastern Alaska involve some amount of right-lateral strike slip eastward of the Sitka Graywacke. The Border Ranges Fault bounds the east side of the Chugach terrane, and speculations on the amount of right slip range from hundreds of kilometers to more than 1,000 km (Smart and others, 1996; Roeske and others, 2003). The slip must have occurred before 50 m.y., when a pluton intruded across the fault on Chichagof Island (Johnson and Karl, 1985, L.W. Snee, written commun., 1997). The Chatham Strait Fault has ~150 km of right slip (see discussion in Hudson and others, 1982). The Tintina Fault in British Columbia has ~420 km of right slip (Gabrielse, 1985) that likely occurred in early Tertiary time (Jackson and Mortensen, 2000). The eastern Denali Fault has ~370 km of right-lateral offset (Lowey, 1998). Thus, significant margin-parallel right slip clearly occurred in the interval between deposition of the Sitka Graywacke and ~50 m.y., after which major activity ceased on all these fault systems except the Chatham Strait Fault. Regardless of the uncertainties as to how much slip occurred on different faults at particular times, the Sitka Graywacke was situated south of its present position. Therefore, zircon sources in coastal and central to

southern interior British Columbia seem most likely. Although some ages are consistent with source regions in the St. Elias Mountains and in south-central Alaska, they are not demanded.

Period	Series epoch	Stage age	Age (m.y.)
Cretaceous	Upper	Paleocene	58.7 ± 0.2
		Selandian	61.7 ± 0.2
		Danian	65.5 ± 0.3
		Maastrichtian	70.6 ± 0.6
		Campanian	83.5 ± 0.2
		Santonian	85.8 ± 0.7
		Coniacian	89.3 ± 1.0
	Lower	Turonian	93.5 ± 0.8
		Cenomanian	99.6 ± 0.9
		Albian	112.0 ± 1.0
		Aptian	125.0 ± 1.0
		Barremian	130.0 ± 1.5
		Hauterivian	136.4 ± 2.0
		Valanginian	140.2 ± 3.0
		Berriasian	145.5 ± 4.0

Youngest detrital-zircon peak ages from samples of Sitka Graywacke

Upper part of the Yakutat Group

Valdez Group

PWSSA

McHugh Complex

Kelp Bay Group

Figure 6. Age range for the Valdez Group (Tysdal and Plafker, 1978, Winkler, 1992; Plafker and others, 1994), younger part of the Kelp Bay Group (Plafker and others, 1976, Decker, 1980), and the McHugh Complex (Winkler, 1992; Plafker and others, 1994), fossiliferous rocks of central Prince William Sound (PWSSA [Prince William Sound Special Study Area]; Nelson and others, 1999), “upper” flysch facies of the Yakutat Group (Jones and Clark, 1973, W.V. Sliter, in Rau and others, 1983), and detrital-zircon youngest peak ages for the Sitka Graywacke (this study). Time scale from Gradstein and others (2005).

Acknowledgments

Discussions with Jeff Trop and Dwight Bradley aided our interpretation of the provenance data; their reviews of the manuscript were also greatly appreciated, as were comments by Maria Luisa Crawford and Rich Goldfarb. Thanks also to Alex Pullen for his assistance in processing the U-Pb geochronologic samples. The U-Pb geochronology was supported by National Science Foundation grants EAR-9526263 and EAR-0309885.

References Cited

- Berg, H.C., and Hinckley, D.W., 1963, Reconnaissance geology of northern Baranof Island, Alaska, *in* Contributions to general geology, 1961: U.S. Geological Survey Bulletin 1141-O, p. O1–O24 [includes geologic map, scale 1:125,000].
- Breitsprecher, Katrin, and Mortensen, J.K., 2004a, BCAGe 2004A—1—a database of isotopic age determinations for rock units from British Columbia: British Columbia Geological Survey Open File 2004–3 [release 3.0].
- Breitsprecher, Katrin, and Mortensen, J.K., 2004b, YukonAge 2004; a database of isotopic age determinations for rock units from Yukon Territory: Whitehorse, Yukon Territory, Canada, Yukon Geological Survey [CD-ROM].
- Butler, R.F., Gehrels, G.E., Hart, William, Davidson, Cameron, and Crawford, M.L., in press, Paleomagnetism of Late Jurassic to mid-Cretaceous plutons near Prince Rupert, British Columbia, *in* Haggart, J.W., Enkin, R.J., and Monger, J.W.H., eds., Paleogeography of western North America; constraints on large-scale latitudinal displacements: Geological Association of Canada Special Paper.
- Crawford, M.L., Crawford, W.A., and Gehrels, G.E., 2000, Terrane assembly and structural relationships in the eastern Prince Rupert quadrangle, British Columbia, *in* Stowell, H.H., and McClelland, W.C., eds., Tectonics of the Coast Mountains, southern Alaska and British Columbia: Geological Society of America Special Paper 343, p. 1–21.
- Davis, S.J., Roeske, S.M., and Karl, S.M., 1998, Late Cretaceous to early Tertiary transtension and strain partitioning in the Chugach accretionary complex, SE Alaska: Journal of Structural Geology, v. 20, no. 5, p. 639–654.
- Decker, J.E., 1980, Geology of a Cretaceous subduction complex, western Chichagof Island, southeastern Alaska: Stanford, Calif., Stanford University, Ph.D. thesis, 135 p.
- Decker, John, Nilson, T.H., and Karl, S.M., 1979, Turbidite facies of the Sitka Graywacke, southeastern Alaska, *in* Johnson, K.M., and Williams, J.R., eds., The United States Geological Survey in Alaska; accomplishments during 1978: U.S. Geological Survey Circular 804-B, p. B125–B129.
- Dodds, C.J., and Campbell, R.B., 1988, Potassium-argon ages of mainly intrusive rocks in the Saint Elias Mountains, Yukon and British Columbia: Geological Survey of Canada Paper 87–16, 43 p.
- Gabrielse, Hubert, 1985, Major dextral transcurrent displacements along the northern Rocky Mountain Trench and related lineaments in north-central British Columbia: Geological Society of America Bulletin, v. 96, no. 1, p. 1–14.
- Gehrels, G.E., 2000, Reconnaissance geology and U-Pb geochronology of the west flank of the Coast Mountains between Juneau and Skagway, southeastern Alaska, *in* Stowell, H.H., and McClelland, W.C., eds., Tectonics of the Coast Mountains, southern Alaska and British Columbia: Geological Society of America Special Paper 343, p. 213–233.
- Gehrels, G.E., 2001, Geology of the Chatham Sound region, Southeast Alaska and coastal British Columbia: Canadian Journal of Earth Sciences, v. 38, no. 11, p. 1579–1599.
- Gradstein, F.M., Ogg, J.G., and Smith, A.G., 2005, A geologic time scale 2004: London, Cambridge University Press, 610 p.
- Grant, U.S., and Higgins, D.F., 1910, Reconnaissance of the geology and mineral resources of Prince William Sound, Alaska: U.S. Geological Survey Bulletin 443, 89 p. [includes geologic map, scale 1:250,000].
- Haeussler, P.J., and Nelson, S.W., 1993, Structural evolution of the Chugach-Prince William Terrane at the hinge of the orocline in Prince William Sound, and implications for ore deposits, *in* Dusel-Bacon, Cynthia, and Till, A.B., eds., Geologic studies in Alaska by the U.S. Geological Survey in 1992: U.S. Geological Survey Bulletin 2068, p. 143–162.
- Hollister, L.S., 1982, Metamorphic evidence for rapid (2 mm/yr) uplift of a portion of the Central Gneiss Complex, Coast Mountains, B.C.: Canadian Mineralogist, v. 20, no. 3, p. 319–332.
- Hudson, Travis, Plafker, George, and Dixon, Kirk, 1982, Horizontal offset history of the Chatham Strait fault, *in* Coonrad, W.L., ed., The United States Geological Survey in Alaska; accomplishments during 1980: U.S. Geological Survey Circular 844, p. 128–132.
- Jackson, L.E., Jr., and Mortensen, J.K., 2000, New constraints indicate mainly early Paleogene displacement on the Tintina fault zone in the northern Cordillera [abs.]: Geological Society of America Abstracts with Programs, v. 32, no. 6, p. 21.

10 Constraints on the Age and Provenance of the Chugach Accretionary Complex, Alaska

- Johnson, B.R., and Karl, S.M., 1985, Geologic map of western Chichagof and Yakobi Islands, southeastern Alaska: U.S. Geological Survey Miscellaneous Investigations Map I-1506, 15 p., scale 1:125,000.
- Jones, D.L., and Clark, S.H.B., 1973, Upper Cretaceous (Maestrichtian) fossils from the Kenai-Chugach mountains, Kodiak and Shumagin Islands, southern Alaska: U.S. Geological Survey Journal of Research, v. 1, no. 2, p. 125–136.
- Kapp, P.A., and Gehrels, G.E., 1998, Detrital zircon constraints on the tectonic evolution of the Gravina Belt, Southeastern Alaska: Canadian Journal of Earth Sciences, v. 35, no. 3, p. 253–268.
- Karl, S.K., Haeussler, P.J., Himmelberg, Glenn, and Zumsteg, C.Z., in press, Geologic map of Baranof Island, Alaska: U.S. Geological Survey Scientific Investigations Map, scale 1:250,000.
- Loney, R.A., Berg, H.C., Pomeroy, J.S., and Brew, D.A., 1963, Reconnaissance geologic map of Chichagof Island and northwestern Baranof Island, Alaska: U.S. Geological Survey Miscellaneous Geologic Investigations Map I-388, scale 1:250,000.
- Lowey, G.W., 1998, A new estimate of the amount of displacement on the Denali Fault system based on the occurrence of carbonate megaboulders in the Dezadeash Formation (Jura-Cretaceous), Yukon, and the Nutzotin Mountains Sequence (Jura-Cretaceous), Alaska: Bulletin of Canadian Petroleum Geology, v. 46, no. 3, p. 379–386.
- Ludwig, K.R., 2003, User's manual for Isoplot 3.0: a geochronological toolkit for Microsoft Excel: Berkeley, Calif., Berkeley Geochronology Center Special Publication 4, 71 p.
- McClelland, W.C., and Mattinson, J.M., 2000, Cretaceous-Tertiary evolution of the western Coast Mountains, central southeastern Alaska, in Stowell, H.H., and McClelland, W.C., eds., Tectonics of the Coast Mountains, southern Alaska and British Columbia: Geological Society of America Special Paper 343, p. 159–182.
- Miller, T.P., 1994, Pre-Cenozoic plutonic rocks in mainland Alaska, in Plafker, George, and Berg, H.C., eds., The geology of Alaska, v. G-1 of The geology of North America: Boulder, Colo., Geological Society of America, p. 535–554.
- Moll-Stalcup, E.J., Brew, D.A., and Vallier, T.L., 1994, Latest Cretaceous and Cenozoic magmatic rocks of Alaska, in Plafker, George, and Berg, H.C., eds., The geology of Alaska, v. G-1 of The geology of North America: Boulder, Colo., Geological Society of America, scale 1:2,500,000.
- Nelson, S.W., Dumoulin, J.A., and Miller, M.L., 1985, Geologic map of the Chugach National Forest, Alaska: U.S. Geological Survey Miscellaneous Field Studies Map MF-1645-B, 16 p., scale 1:250,000.
- Nelson, S.W., Miller, M.L., Haeussler, P.J., Snee, L.W., Phillips, P.J., and Huber, Carol, 1999, Preliminary geologic map of the Chugach National Forest special study area, Alaska: U.S. Geological Survey Open-File Report 99-362, scale 1:63,360 [<http://wrgis.wr.usgs.gov/open-file/of99-362/>].
- Nilsen, T.H., 1984, Trench-fill submarine-fan associations of the Upper Cretaceous Chugach terrane, southern Alaska: Geo-Marine Letters, v. 3, no. 2–4, p. 179–185.
- Nilsen, T.H., and Moore, G.W., 1979, Reconnaissance study of Upper Cretaceous to Miocene stratigraphic units and sedimentary facies, Kodiak and adjacent islands, Alaska: U.S. Geological Survey Professional Paper 1093, 34 p.
- Nilson, T.H., and Zuffa, G.G., 1982, The Chugach terrane, a Cretaceous trench-fill deposit southern Alaska, in Leggett, J.K., ed., Trench-forearc geology—sedimentation and tectonics on modern and ancient active plate margins: Geological Society of London, Special Publication 10, p. 213–227.
- Nokleberg, W.J., West, T.D., Dawson, K.M., Shpkerman, V.I., Bundtzen, T.K., Parfenov, L.M., Monger, J.W.H., Ratkin, V.V., Baranov, B.V., Byalobzhesky, S.G., Diggles, M.F., Eremin, R.A., Fugita, Kazuga, Gordey, S.P., Gorodinskiy, M.E., Goryachev, N.A., Feeney, T.D., Frolov, T.F., Grantz, Arthur, Khanchuk, A.I., Koch, R.D., Natalin, B.A., Nata-pov, L.M., Norton, I.O., Patton, W.W., Jr., Plafker, George, Pozdeev, A.I., Rozenblum, I.S., Scholl, D.W., Sokolov, S.D., Sosunov, G.M., Stone, D.B., Tabor, R.W., Tsukanov, N.V., and Vallier, T.L., 1998, Summary terrane, mineral deposit, and metallogenic belt maps of the Russian Far East, Alaska, and the Canadian Cordillera: U.S. Geological Survey Open-File Report 98-136, CD-ROM [<http://wrgis.wr.usgs.gov/open-file/of98-136/>].
- Plafker, George, Hudson, Travis, Bruns, T.R., and Rubin, Meyer, 1978, Late Quaternary offsets along the Fairweather fault and crustal plate interactions in southern Alaska: Canadian Journal of Earth Sciences, v. 15, no. 5, p. 805–816.
- Plafker, George, Jones, D.L., Hudson, Travis, and Berg, H.C., 1976, The Border Ranges Fault system in the Saint Elias Mountains and Alexander Archipelago, in Cobb, E.H., ed., The United States Geological Survey in Alaska; accomplishments during 1975: U.S. Geological Survey Circular 733, p. 14–16.

- Plafker, George, Nokleberg, W.J., and Lull, J.S., 1989, Bedrock geology and tectonic evolution of the Wrangellia, Peninsular, and Chugach terranes along the Trans-Alaska Crustal Transect in the Chugach Mountains and southern Copper River basin, Alaska: *Journal of Geophysical Research*, v. 94, no. B4, p. 4255–4295.
- Plafker, George, Jones, D.L., and Pessagno, E.A., Jr., 1977, A Cretaceous accretionary flysch and mélange terrane along the Gulf of Alaska margin, in Blean, K.M., ed., *The United States Geological Survey in Alaska—accomplishments during 1976*: U.S. Geological Survey Circular 751-B, p. B41–B43.
- Plafker, George, Moore, J.C., and Winkler, G.R., 1994, Geology of the southern Alaska margin, in Plafker, George, and Berg, H.C., eds., *The geology of Alaska*, v. G-1 of *The geology of North America*: Boulder, Colo., Geological Society of America, p. 389–449.
- Rau, W.W., Plafker, George, and Winkler, G.R., 1983, Foraminiferal biostratigraphy and correlations in the Gulf of Alaska Tertiary province: U.S. Geological Survey Oil and Gas Investigations Chart 120, 11 p., 3 sheets.
- Reifenstuhl, R.R., 1986, Geology of the Goddard Hot Springs area, Baranof Island, southeastern Alaska: Alaska Division of Geological and Geophysical Surveys Public-Data File 86–2, 82 p.
- Roeske, S.M., Snee, L.W., and Pavlis, T.L., 2003, Dextral-slip reactivation of an arc-forearc boundary during Late Cretaceous-Early Eocene oblique convergence in the northern Cordillera, in Sisson, V.B., Roeske, S.M., and Pavlis, T.L., eds., *Geology of a transpressional orogen developed during ridge-trench interaction along the North Pacific margin*: Geological Society of America Special Paper 371, p. 141–169.
- Sample, J.C., and Moore, J.C., 1987, Structural style and kinematics of an underplated slate belt, Kodiak and adjacent islands, Alaska: *Geological Society of America Bulletin*, v. 99, no. 1, p. 7–20.
- Smart, K.J., Pavlis, T.L., Sisson, V.B., Roeske, S.M., and Snee, L.W., 1996, The Border Ranges fault system in Glacier Bay National Park, Alaska; evidence for major early Cenozoic dextral strike-slip motion: *Canadian Journal of Earth Sciences*, v. 33, no. 9, p. 1268–1282.
- Stacey, J.S., and Kramers, J.D., 1975, Approximation of terrestrial lead isotope evolution by a two-stage model: *Earth and Planetary Science Letters*, v. 26, no. 2, p. 207–221.
- Tarr, R.S., and Butler, B.S., 1909, The Yakutat Bay region, Alaska: U.S. Geological Survey Professional Paper 64, 183 p.
- Trop, J.M., Szuch, D.A., Rioux, Matthew, and Blodgett, R.B., 2005, Sedimentology and provenance of the Upper Jurassic Naknek Formation, Talkeetna Mountains, Alaska; bearings on the accretionary tectonic history of the Wrangellia composite terrane: *Geological Society of America Bulletin*, v. 117, no. 5–6, p. 570–588.
- Tysdal, R.G., and Plafker, George, 1978, Age and continuity of the Valdez Group, southern Alaska, in Sohl, N.F., and Wright, W.B., eds., *Changes in stratigraphic nomenclature by the U.S. Geological Survey, 1977*: U.S. Geological Survey Bulletin 1457-A, p. A120–A124.
- van der Heyden, Peter, 1992, A Middle Jurassic to early Tertiary Andean-Sierran arc model for the Coast Belt of British Columbia: *Tectonics*, v. 11, no. 1, p. 82–97.
- Winkler, G.R., 1992, Geologic map and summary geochronology of the Anchorage 1°×3° quadrangle, southern Alaska: U.S. Geological Survey Miscellaneous Investigations Map I-2283, scale 1:250,000.
- Winkler, G.R., Silberman, M.L., Grantz, Arthur, Miller, R.J., and MacKevett, E.M., Jr., 1980, Geologic map and summary geochronology of the Valdez quadrangle, southern Alaska: U.S. Geological Survey Open-File Report 80-892-A, 2 sheets, scale 1:250,000.

Table 2

Table 2. Analytical data on detrital zircons

[All analyses by laser-ablation inductively coupled plasma mass spectroscopy (ICPMS)]

Analysis	U content (ppm)	$^{206}\text{Pb}/^{204}\text{Pb}$ ratio	U/Th ratio	$^{206}\text{Pb}/^{208}\text{Pb}$ ratio	\pm (pct)	$^{205}\text{Pb}/^{235}\text{U}$ ratio	\pm (pct)	$^{206}\text{Pb}/^{207}\text{Pb}$ ratio	\pm (pct)	Error correlation	$^{206}\text{Pb}/^{238}\text{U}$ age (m.y.)	\pm (m.y.)	$^{207}\text{Pb}/^{235}\text{U}$ age (m.y.)	\pm (m.y.)	$^{206}\text{Pb}/^{207}\text{Pb}$ age (m.y.)	\pm (m.y.)
<i>Sample 62</i>																
1	174	1,518	45	0.01036	0.5	0.06271	6.1	22.77	6.1	0.08	66.4	0.3	61.8	3.9	-115	75
2	167	1,277	29	0.01097	1.6	0.07066	6.7	21.41	6.6	0.23	70.4	1.1	69.3	4.8	34	78
3	106	5,285	32	0.03082	1.6	0.20209	5.1	21.03	4.8	0.31	195.7	3.1	186.9	10.3	77	57
4	205	3,040	49	0.01328	1.5	0.08855	3.7	20.67	3.4	0.40	85.0	1.3	86.2	3.3	118	40
5	116	1,426	24	0.03218	1.0	0.25335	3.6	17.51	3.5	0.27	204.2	2.0	229.3	9.3	495	38
6	182	1,575	50	0.01736	1.7	0.11639	2.7	20.56	2.1	0.62	110.9	1.9	111.8	3.1	130	25
7	624	5,499	40	0.01156	0.6	0.07674	2.2	20.77	2.1	0.28	74.1	0.5	75.1	1.7	106	25
8	58	10,610	14	0.26190	1.2	3.73401	1.4	9.67	0.7	0.88	1,499.6	20.2	1,578.7	50.6	1,686	6
9	310	1,947	13	0.01388	1.8	0.09780	4.0	19.58	3.5	0.45	88.9	1.6	94.7	3.9	245	41
10	582	3,858	25	0.01246	2.0	0.09618	2.6	17.87	1.7	0.76	79.8	1.6	93.2	2.5	451	19
11	48	626	32	0.01187	2.1	0.05028	4.5	32.55	4.0	0.46	76.1	1.6	49.8	2.3	-1,087	61
12	115	2,152	48	0.01271	0.7	0.08244	6.3	21.25	6.2	0.11	81.4	0.6	80.4	5.2	52	74
13	575	5,485	23	0.01105	0.6	0.07384	2.6	20.64	2.6	0.23	70.9	0.4	72.3	2.0	122	30
14	55	618	24	0.01126	1.8	0.04703	25.7	33.01	25.7	0.07	72.2	1.3	46.7	12.2	-1,129	392
15	240	1,712	21	0.01544	1.1	0.10393	3.4	20.49	3.2	0.31	98.8	1.1	100.4	3.5	139	38
16	64	610	65	0.01195	2.7	0.05233	7.7	31.49	7.1	0.36	76.6	2.1	51.8	4.1	-988	106
17	916	7,112	53	0.01207	1.0	0.08152	1.4	20.42	1.1	0.66	77.4	0.7	79.6	1.2	146	13
18	272	3,812	21	0.01434	1.6	0.08823	2.7	22.41	2.2	0.59	91.8	1.5	85.9	2.4	-76	27
19	342	4,617	12	0.01512	0.7	0.10298	2.8	20.24	2.7	0.26	96.7	0.7	99.5	2.9	167	32
20	79	1,714	101	0.02309	2.9	0.14268	6.2	22.32	5.5	0.46	147.2	4.3	135.4	8.9	-66	67
21	140	1,036	120	0.01220	1.4	0.08865	6.7	18.98	6.6	0.21	78.2	1.1	86.2	6.0	316	75
22	220	2,789	49	0.01404	1.1	0.09104	3.7	21.26	3.5	0.30	89.9	1.0	88.5	3.4	51	42
23	514	6,619	22	0.01091	1.2	0.07533	3.6	19.96	3.4	0.35	69.9	0.9	73.7	2.7	199	39
24	89	12,945	17	0.27611	1.1	3.95064	1.4	9.64	0.9	0.79	1,571.8	19.3	1,624.1	53.9	1,693	8
25	410	3,986	10	0.01359	9.1	0.09969	10.2	18.79	4.7	0.89	87.0	7.9	96.5	10.3	338	54
26	378	3,213	74	0.01387	2.7	0.10538	4.0	18.15	2.9	0.68	88.8	2.4	101.7	4.2	417	32
27	184	2,040	48	0.01233	0.8	0.08421	6.9	20.20	6.8	0.12	79.0	0.7	82.1	5.9	172	80
28	161	3,923	28	0.02912	1.2	0.20582	3.2	19.51	2.9	0.39	185.0	2.3	190.0	6.6	253	33
29	174	1,501	27	0.01535	1.0	0.12429	6.9	17.03	6.8	0.15	98.2	1.0	119.0	8.6	557	74
30	515	3,856	35	0.01111	1.0	0.07611	2.3	20.13	2.1	0.43	71.2	0.7	74.5	1.8	180	24
31	756	3,662	13	0.01062	2.3	0.07743	3.6	18.91	2.7	0.64	68.1	1.6	75.7	2.8	324	31
32	80	853	58	0.01213	3.1	0.07814	13.7	21.41	13.3	0.23	77.8	2.4	76.4	10.8	34	160
33	131	1,278	39	0.01219	1.4	0.08371	8.0	20.08	7.9	0.18	78.1	1.1	81.6	6.8	186	92
34	83	1,114	47	0.01191	1.9	0.10958	10.2	14.99	10.0	0.19	76.3	1.5	105.6	11.2	829	104
35	37	498	26	0.01153	1.4	0.06054	16.7	26.26	16.7	0.08	73.9	1.0	59.7	10.2	-479	221
36	92	64,668	54	0.01061	2.1	0.10404	26.4	14.06	26.3	0.08	68.0	1.4	100.5	27.5	961	268
37	124	1,304	38	0.01492	1.6	0.12926	10.1	15.92	10.0	0.15	95.5	1.5	123.4	13.2	702	106
38	175	546	48	0.01430	1.9	0.10767	6.3	18.32	6.0	0.31	91.5	1.8	103.8	6.9	396	67
39	77	410	62	0.01124	3.2	0.06565	7.8	23.62	7.2	0.41	72.1	2.3	64.6	5.2	-206	90
40	63	513	37	0.01082	0.7	0.04868	15.1	30.66	15.1	0.05	69.4	0.5	48.3	7.4	-909	219
41	146	5,387	142	0.01342	2.4	0.10595	6.1	17.47	5.6	0.39	86.0	2.1	102.3	6.6	501	62
42	102	1,368	45	0.01311	1.7	0.09386	11.7	19.26	11.6	0.15	84.0	1.5	91.1	11.1	282	133
43	238	951	39	0.01135	0.6	0.09435	5.6	16.59	5.6	0.11	72.8	0.5	91.5	5.4	614	60
44	177	1,516	24	0.01164	0.7	0.07871	5.9	20.39	5.9	0.11	74.6	0.5	76.9	4.7	150	69
45	147	1,171	29	0.01183	0.8	0.07098	7.0	22.99	6.9	0.12	75.8	0.6	69.6	5.0	-139	86
46	349	2,642	16	0.01548	0.5	0.11711	3.8	18.22	3.8	0.13	99.0	0.5	112.4	4.5	407	42

Table 2. Analytical data on detrital zircons.—Continued

[All analyses by laser-ablation inductively coupled plasma mass spectroscopy (ICPMS)]

Analysis	U content (ppm)	$^{206}\text{Pb}/^{204}\text{Pb}$ ratio	U/Th ratio	$^{206}\text{Pb}/^{208}\text{Pb}$ ratio	\pm (pct)	$^{205}\text{Pb}/^{235}\text{U}$ ratio	\pm (pct)	$^{206}\text{Pb}/^{207}\text{Pb}$ ratio	\pm (pct)	Error correlation	$^{206}\text{Pb}/^{238}\text{U}$ age (m.y.)	\pm (m.y.)	$^{207}\text{Pb}/^{235}\text{U}$ age (m.y.)	\pm (m.y.)	$^{206}\text{Pb}/^{207}\text{Pb}$ age (m.y.)	\pm (m.y.)
47	244	8,934	65	0.06705	1.4	0.51139	1.5	18.08	0.7	0.90	418.4	5.9	419.4	7.8	425	7
48	344	3,790	23	0.01685	1.2	0.12062	2.3	19.26	2.0	0.52	107.7	1.3	115.6	2.8	282	23
49	315	3,063	32	0.01545	0.9	0.10319	3.5	20.65	3.3	0.27	98.9	0.9	99.7	3.6	120	39
50	135	1,401	25	0.01501	0.7	0.08852	6.1	23.39	6.0	0.11	96.1	0.7	86.1	5.4	-182	75
51	133	1,689	34	0.01554	1.7	0.11988	10.1	17.87	10.0	0.17	99.4	1.7	115.0	12.3	451	111
52	119	1,630	32	0.02311	1.8	0.15298	4.7	20.83	4.4	0.38	147.3	2.6	144.5	7.3	99	52
53	108	728	63	0.01455	3.0	0.11625	8.1	17.25	7.5	0.37	93.1	2.8	111.7	9.5	528	82
54	45	689	41	0.01399	3.4	0.12501	17.2	15.43	16.8	0.20	89.6	3.1	119.6	21.6	768	177
55	1,139	4,694	29	0.01146	0.9	0.07642	1.8	20.67	1.5	0.52	73.4	0.7	74.8	1.4	118	18
56	453	2,568	20	0.01071	0.6	0.06663	2.5	22.16	2.4	0.24	68.7	0.4	65.5	1.7	-49	29
57	160	899	35	0.01525	0.9	0.10584	4.2	19.87	4.1	0.21	97.6	0.8	102.2	4.5	211	47
58	267	2,332	43	0.01237	0.8	0.08554	3.5	19.94	3.5	0.22	79.3	0.6	83.3	3.1	202	40
59	186	1,509	41	0.01330	3.2	0.08058	6.1	22.76	5.1	0.53	85.2	2.8	78.7	4.9	-115	63
60	199	896	51	0.01226	2.0	0.06797	5.3	24.87	4.9	0.37	78.6	1.6	66.8	3.7	-338	63
61	187	1,285	46	0.01390	2.3	0.10999	8.1	17.42	7.7	0.29	89.0	2.1	106.0	8.9	507	85
62	319	4,204	20	0.01743	3.0	0.12210	4.2	19.69	2.9	0.71	111.4	3.3	117.0	5.1	232	34
63	421	2,707	40	0.01114	0.6	0.07046	2.7	21.81	2.6	0.24	71.4	0.5	69.1	1.9	-10	32
64	324	2,778	33	0.01456	0.7	0.09647	2.5	20.81	2.4	0.28	93.2	0.7	93.5	2.5	102	29
65	180	1,060	26	0.01052	0.7	0.07889	6.3	18.39	6.3	0.12	67.5	0.5	77.1	5.0	386	70
66	337	1,929	20	0.01432	0.7	0.10075	3.2	19.59	3.2	0.20	91.6	0.6	97.5	3.3	243	36
67	220	970	41	0.01173	1.3	0.09427	6.2	17.16	6.0	0.21	75.2	1.0	91.5	5.9	540	66
68	164	1,344	40	0.01514	2.0	0.10335	6.6	20.19	6.2	0.31	96.8	2.0	99.9	6.9	173	73
69	437	1,811	-2	0.01085	1.0	0.06058	5.4	24.69	5.3	0.19	69.6	0.7	59.7	3.3	-319	68
70	252	2,273	23	0.01512	1.0	0.10903	4.7	19.13	4.6	0.21	96.8	0.9	105.1	5.2	298	53

Sample 63

1	59	13,918	31	0.02270	0.8	0.15078	9.0	20.76	8.9	0.09	144.7	1.2	142.6	13.6	108	105
2	160	5,137	28	0.01111	1.0	0.07275	5.1	21.05	5.0	0.19	71.2	0.7	71.3	3.8	74	59
3	238	3,161	149	0.01107	0.7	0.06868	2.7	22.21	2.6	0.25	70.9	0.5	67.4	1.8	-55	31
4	22	573	43	0.01313	1.6	0.07440	25.5	24.34	25.5	0.06	84.1	1.3	72.9	19.1	-282	324
5	79	5,831	36	0.06016	0.7	0.47700	2.5	17.39	2.4	0.28	376.6	2.7	396.0	11.8	511	26
6	25	1,964	20	0.01481	0.9	0.07898	19.1	25.85	19.1	0.05	94.7	0.9	77.2	15.2	-438	251
7	37	83,222	9	0.32258	0.9	4.92856	3.7	9.02	3.6	0.24	1,802.3	18.2	1,807.2	169.0	1,813	32
8	72	1,342	56	0.01240	1.4	0.11052	16.5	15.46	16.4	0.09	79.4	1.1	106.4	18.3	763	173
9	173	7,344	27	0.01107	0.8	0.07715	7.2	19.79	7.2	0.10	71.0	0.5	75.5	5.6	219	83
10	139	3,192	66	0.01263	1.4	0.08372	4.2	20.81	3.9	0.33	80.9	1.1	81.6	3.5	102	46
12	48	5,639	-149	0.02344	1.7	0.15879	5.6	20.35	5.3	0.31	149.4	2.6	149.6	8.9	154	62
13	104	23,808	37	0.01282	0.6	0.10712	17.4	16.50	17.4	0.04	82.1	0.5	103.3	18.8	625	188
14	471	10,746	25	0.01079	0.7	0.07227	1.9	20.59	1.8	0.35	69.2	0.5	70.9	1.4	128	21
15	119	28,627	31	0.01178	1.0	0.09242	14.5	17.57	14.4	0.07	75.5	0.7	89.8	13.5	488	159
16	131	12,296	31	0.01130	1.0	0.07432	7.6	20.97	7.5	0.13	72.5	0.7	72.8	5.7	84	89
17	181	3,725	29	0.03062	0.5	0.20932	2.7	20.17	2.6	0.19	194.4	1.0	193.0	5.7	175	31
18	48	5,001	103	0.01248	1.7	0.12078	18.2	14.25	18.1	0.09	80.0	1.4	115.8	22.0	933	185
19	112	1,125	58	0.01337	1.8	0.07625	3.8	24.18	3.4	0.47	85.6	1.5	74.6	3.0	-265	43
20	483	5,095	22	0.01113	0.6	0.07776	3.4	19.73	3.3	0.17	71.3	0.4	76.0	2.7	226	38
21	214	3,919	139	0.01438	1.1	0.12694	3.6	15.62	3.4	0.31	92.0	1.0	121.3	4.6	743	36
22	134	1,873	37	0.01101	0.9	0.07754	5.3	19.58	5.2	0.17	70.6	0.6	75.8	4.2	244	60

Table 2. Analytical data on detrital zircons.—Continued

[All analyses by laser-ablation inductively coupled plasma mass spectroscopy (ICPMS)]

Analysis	U content (ppm)	$^{206}\text{Pb}/^{204}\text{Pb}$ ratio	U/Th ratio	$^{206}\text{Pb}/^{208}\text{Pb}$ ratio	\pm (pct)	$^{205}\text{Pb}/^{235}\text{U}$ ratio	\pm (pct)	$^{206}\text{Pb}/^{207}\text{Pb}$ ratio	\pm (pct)	Error correlation	$^{206}\text{Pb}/^{238}\text{U}$ age (m.y.)	\pm (m.y.)	$^{207}\text{Pb}/^{235}\text{U}$ age (m.y.)	\pm (m.y.)	$^{206}\text{Pb}/^{207}\text{Pb}$ age (m.y.)	\pm (m.y.)
23	177	8,126	29	0.01192	0.7	0.07867	6.9	20.89	6.8	0.10	76.4	0.5	76.9	5.5	92	81
24	51	4,372	25	0.01652	1.5	0.11365	11.2	20.04	11.1	0.13	105.6	1.6	109.3	12.8	191	129
25	294	7,446	47	0.01150	2.9	0.07741	4.3	20.49	3.2	0.66	73.7	2.1	75.7	3.4	139	38
26	263	8,458	72	0.01466	1.2	0.09323	2.7	21.68	2.4	0.44	93.8	1.1	90.5	2.5	4	29
27	33	1,099	51	0.02267	1.9	0.16385	19.7	19.07	19.7	0.10	144.5	2.8	154.1	32.3	304	224
28	111	104,314	33	0.01125	1.3	0.08231	35.5	18.85	35.5	0.04	72.1	1.0	80.3	29.2	331	402
29	78	3,743	29	0.05339	0.7	0.40188	2.6	18.32	2.5	0.26	335.3	2.3	343.0	10.4	396	28
30	83	2,866	25	0.01235	1.0	0.08878	10.7	19.19	10.7	0.10	79.1	0.8	86.4	9.6	291	122
31	78	1,113	36	0.01086	1.1	0.06350	7.6	23.58	7.5	0.14	69.6	0.8	62.5	4.9	-203	94
32	105	16,364	29	0.01155	0.9	0.07634	8.3	20.87	8.3	0.11	74.0	0.7	74.7	6.4	96	98
33	135	1,304	-4	0.01208	1.9	0.05835	7.7	28.54	7.5	0.24	77.4	1.5	57.6	4.6	-706	104
34	144	15,149	18	0.05467	1.1	0.40752	2.0	18.50	1.7	0.53	343.1	3.7	347.1	8.3	374	19
35	90	1,311	43	0.01139	1.0	0.05916	8.0	26.55	8.0	0.12	73.0	0.7	58.4	4.8	-508	106
36	165	7,645	16	0.01221	0.8	0.08735	5.5	19.27	5.4	0.15	78.2	0.6	85.0	4.9	281	62
37	69	778	55	0.01411	1.0	0.06097	7.0	31.91	6.9	0.15	90.3	0.9	60.1	4.3	-1027	102
38	604	3,928	34	0.01150	0.7	0.07040	2.9	22.52	2.8	0.26	73.7	0.6	69.1	2.0	-88	34
39	285	4,345	12	0.02867	2.1	0.21587	3.3	18.31	2.6	0.62	182.2	3.8	198.5	7.3	396	29
40	121	3,609	42	0.01198	0.9	0.14225	3.9	11.61	3.8	0.22	76.8	0.7	135.0	5.6	1,341	36
41	83	2,687	27	0.01118	0.6	0.07305	6.3	21.10	6.3	0.09	71.6	0.4	71.6	4.7	69	75
42	40	3,714	27	0.02385	2.1	0.14782	18.1	22.24	18.0	0.12	151.9	3.2	140.0	26.8	-58	219
43	172	4,776	102	0.01479	2.1	0.14146	5.5	14.42	5.1	0.38	94.7	2.0	134.3	7.9	909	52
44	82	1,327	63	0.01846	2.0	0.10719	6.4	23.74	6.1	0.31	117.9	2.3	103.4	7.0	-220	77
45	473	7,172	33	0.01129	0.5	0.07470	2.2	20.84	2.2	0.23	72.4	0.4	73.1	1.7	99	26
46	58	2,165	26	0.01164	1.3	0.06051	12.4	26.52	12.3	0.10	74.6	0.9	59.7	7.6	-505	164
47	90	7,619	31	0.01207	1.1	0.08245	10.8	20.19	10.7	0.10	77.4	0.9	80.4	9.0	173	125
48	50	2,388	22	0.01154	1.1	0.07187	14.8	22.13	14.8	0.08	73.9	0.8	70.5	10.7	-46	179
49	123	1,114	49	0.01061	0.9	0.07244	6.9	20.19	6.9	0.13	68.0	0.6	71.0	5.1	173	80
50	66	5,583	27	0.03129	1.0	0.19217	5.0	22.45	4.9	0.19	198.6	1.9	178.5	9.8	-80	60
51	90	5,745	18	0.06100	1.5	0.44518	2.4	18.89	1.9	0.62	381.7	5.8	373.9	10.7	326	21
52	108	1,193	23	0.01128	0.9	0.05842	7.5	26.63	7.4	0.12	72.3	0.6	57.7	4.4	-517	99
53	120	49,185	42	0.06153	0.8	0.47921	4.7	17.70	4.7	0.16	384.9	3.0	397.5	22.8	472	52
54	190	837	17	0.01181	1.2	0.08156	5.9	19.96	5.8	0.20	75.7	0.9	79.6	4.9	200	67
55	38	1,119	23	0.01232	1.8	0.08867	35.1	19.16	35.1	0.05	78.9	1.4	86.3	31.1	294	401
56	155	18,802	29	0.03050	0.6	0.20881	2.8	20.14	2.8	0.21	193.7	1.2	192.6	6.0	179	32
57	109	896	42	0.01132	1.4	0.06251	4.2	24.96	4.0	0.34	72.5	1.0	61.6	2.7	-347	51
58	42	2,803	41	0.02469	2.4	0.15078	7.3	22.58	6.9	0.33	157.2	3.9	142.6	11.2	-95	85
59	25	399	29	0.01263	1.9	0.05939	30.3	29.32	30.2	0.06	80.9	1.5	58.6	18.1	-781	427
60	125	28,732	19	0.02979	0.8	0.21519	4.1	19.09	4.0	0.19	189.2	1.5	197.9	8.9	303	46
61	140	3,849	25	0.01190	1.0	0.07418	6.2	22.11	6.1	0.17	76.2	0.8	72.7	4.6	-43	74
62	56	2,725	30	0.02864	1.1	0.18994	7.4	20.79	7.3	0.15	182.0	2.0	176.6	14.1	105	86
63	135	6,664	46	0.01332	1.4	0.09034	6.3	20.34	6.1	0.22	85.3	1.2	87.8	5.7	156	72
64	50	1,876	73	0.01107	1.6	0.07028	12.9	21.73	12.8	0.12	71.0	1.1	69.0	9.1	-1	154
65	83	1,582	42	0.01147	1.1	0.06950	6.8	22.75	6.7	0.16	73.5	0.8	68.2	4.8	-113	82
66	79	3,213	34	0.02296	1.1	0.15040	3.9	21.05	3.8	0.28	146.3	1.6	142.3	6.0	75	45
67	94	9,235	34	0.05254	0.8	0.39639	2.6	18.28	2.5	0.29	330.1	2.6	339.0	10.6	401	28
68	227	8,155	27	0.01156	0.6	0.07625	6.2	20.90	6.2	0.10	74.1	0.5	74.6	4.8	92	73
69	72	1,239	20	0.05653	1.6	0.37073	5.1	21.03	4.8	0.32	354.5	5.9	320.2	18.9	78	57
70	66	1,449	41	0.01104	2.0	0.06147	12.7	24.77	12.6	0.16	70.8	1.4	60.6	7.9	-327	161

Table 2. Analytical data on detrital zircons.—Continued

[All analyses by laser-ablation inductively coupled plasma mass spectroscopy (ICPMS)]

Analysis	U content (ppm)	$^{206}\text{Pb}/^{204}\text{Pb}$ ratio	U/Th ratio	$^{206}\text{Pb}/^{208}\text{Pb}$ ratio	\pm (pct)	$^{205}\text{Pb}/^{235}\text{U}$ ratio	\pm (pct)	$^{206}\text{Pb}/^{207}\text{Pb}$ ratio	\pm (pct)	Error correlation	$^{206}\text{Pb}/^{238}\text{U}$ age (m.y.)	\pm (m.y.)	$^{207}\text{Pb}/^{235}\text{U}$ age (m.y.)	\pm (m.y.)	$^{206}\text{Pb}/^{207}\text{Pb}$ age (m.y.)	\pm (m.y.)
<i>Sample 64</i>																
1	107	753	38	0.01186	1.3	0.10486	9.6	15.60	9.5	0.14	76.0	1.0	101.3	10.2	745	101
2	82	1,669	22	0.01441	1.4	0.08538	8.5	23.27	8.4	0.16	92.2	1.3	83.2	7.3	-169	104
3	218	3,857	39	0.01150	0.7	0.06840	4.3	23.17	4.2	0.16	73.7	0.5	67.2	3.0	-159	52
4	124	2,154	11	0.01384	1.2	0.09876	5.6	19.32	5.5	0.21	88.6	1.1	95.6	5.6	275	63
5	121	1,671	41	0.01121	1.0	0.06446	7.2	23.98	7.1	0.15	71.9	0.8	63.4	4.7	-245	90
7	188	2,703	25	0.01480	1.4	0.08951	7.0	22.80	6.8	0.21	94.7	1.4	87.0	6.3	-118	84
8	191	1,847	43	0.01212	1.0	0.07342	3.8	22.76	3.6	0.26	77.7	0.8	71.9	2.8	-114	45
9	381	5,374	21	0.01188	0.7	0.08194	3.1	19.98	3.0	0.23	76.1	0.5	80.0	2.5	197	34
10	281	6,578	18	0.01159	1.0	0.07854	4.0	20.34	3.9	0.24	74.3	0.7	76.8	3.2	156	45
11	204	1,007	31	0.01172	1.3	0.06537	4.9	24.73	4.7	0.26	75.1	0.9	64.3	3.2	-323	61
12	316	388	84	0.01178	3.0	0.08824	6.8	18.41	6.0	0.45	75.5	2.3	85.9	6.0	384	68
13	101	5,068	19	0.05417	0.7	0.42835	1.7	17.44	1.6	0.41	340.1	2.5	362.0	7.5	505	17
14	260	4,869	24	0.01409	0.9	0.09759	3.1	19.91	2.9	0.29	90.2	0.8	94.6	3.0	206	34
15	170	1,545	39	0.01402	0.8	0.09165	4.0	21.09	3.9	0.19	89.7	0.7	89.0	3.7	71	47
16	139	1,697	272	0.01685	0.6	0.11463	2.2	20.26	2.1	0.27	107.7	0.7	110.2	2.6	164	25
17	77	1,930	22	0.01619	3.7	0.09738	12.3	22.93	11.8	0.30	103.6	3.8	94.4	12.1	-132	146
18	165	2,164	22	0.01458	0.9	0.09668	3.6	20.79	3.4	0.26	93.3	0.9	93.7	3.5	104	41
19	249	2,812	32	0.01157	2.6	0.07574	5.1	21.06	4.4	0.51	74.2	1.9	74.1	3.9	73	52
20	672	16,092	38	0.01238	1.4	0.08429	2.3	20.25	1.8	0.63	79.3	1.1	82.2	1.9	166	21
21	198	5,005	27	0.01471	0.9	0.10503	4.5	19.31	4.4	0.20	94.2	0.9	101.4	4.7	275	50
22	282	5,660	15	0.01079	0.6	0.07704	5.7	19.32	5.7	0.11	69.2	0.4	75.4	4.5	275	65
23	80	1,490	42	0.01564	2.8	0.10123	10.9	21.30	10.6	0.25	100.0	2.8	97.9	11.2	46	126
24	66	320	116	0.01256	1.5	0.08840	7.9	19.60	7.7	0.19	80.5	1.2	86.0	7.0	242	89
25	172	1,308	63	0.01193	1.0	0.07652	3.9	21.49	3.8	0.25	76.4	0.7	74.9	3.1	25	46
26	250	3,314	51	0.01203	0.8	0.07588	3.7	21.86	3.6	0.22	77.1	0.6	74.3	2.8	-16	43
27	111	11,325	31	0.06624	0.6	0.52233	1.6	17.49	1.5	0.36	413.4	2.4	426.7	8.3	499	16
28	513	4,975	29	0.01172	0.8	0.08892	2.7	18.18	2.6	0.31	75.1	0.6	86.5	2.5	413	29
29	174	1,128	66	0.01146	2.5	0.07198	8.4	21.95	8.0	0.29	73.5	1.8	70.6	6.1	-26	97
30	258	3,501	41	0.01231	1.4	0.07956	3.3	21.33	3.0	0.43	78.9	1.1	77.7	2.7	43	36
31	182	2,851	36	0.01114	0.8	0.07597	7.5	20.22	7.5	0.11	71.4	0.6	74.3	5.8	169	87
32	267	721	84	0.01280	1.3	0.07264	2.3	24.29	1.9	0.56	82.0	1.0	71.2	1.7	-277	24
33	383	5,018	23	0.01473	1.0	0.10927	3.7	18.59	3.6	0.27	94.3	0.9	105.3	4.1	363	40
34	519	5,740	14	0.01111	2.0	0.07778	2.8	19.69	2.0	0.71	71.2	1.4	76.1	2.2	231	23
35	125	1,486	28	0.01784	3.9	0.12643	6.9	19.45	5.7	0.56	114.0	4.4	120.9	8.8	259	66
36	202	3,799	35	0.01321	0.8	0.09898	5.1	18.40	5.0	0.15	84.6	0.7	95.8	5.1	385	56
37	171	1,317	38	0.01492	0.7	0.14103	5.1	14.59	5.0	0.13	95.5	0.6	134.0	7.2	886	52
38	333	1,783	33	0.01134	1.0	0.07609	5.6	20.54	5.5	0.18	72.7	0.7	74.5	4.3	133	65
39	261	6,149	27	0.01151	1.3	0.08247	5.0	19.25	4.8	0.25	73.8	0.9	80.5	4.2	283	55
40	61	1,182	27	0.01435	1.6	0.07682	10.4	25.75	10.3	0.15	91.8	1.5	75.2	8.1	-428	135
41	63	6,499	20	0.05982	0.7	0.44407	2.5	18.57	2.4	0.28	374.5	2.6	373.1	11.1	365	27
42	64	1,397	24	0.01415	5.6	0.10351	16.5	18.85	15.6	0.34	90.6	5.1	100.0	17.2	331	176
43	30	1,061	76	0.01614	3.0	0.09616	12.9	23.15	12.6	0.23	103.2	3.1	93.2	12.5	-156	156
44	367	1,745	71	0.01188	0.8	0.11124	3.9	14.73	3.8	0.21	76.1	0.6	107.1	4.4	866	40
45	460	1,983	89	0.01197	1.1	0.10668	3.1	15.48	2.9	0.34	76.7	0.8	102.9	3.3	762	30
46	133	1,769	28	0.01117	0.9	0.06173	9.7	24.95	9.7	0.09	71.6	0.7	60.8	6.1	-345	124
47	507	7,605	35	0.01138	0.7	0.07780	1.7	20.18	1.5	0.43	73.0	0.5	76.1	1.3	174	18

Table 2. Analytical data on detrital zircons.—Continued

[All analyses by laser-ablation inductively coupled plasma mass spectroscopy (ICPMS)]

Analysis	U content (ppm)	$^{206}\text{Pb}/^{204}\text{Pb}$ ratio	U/Th ratio	$^{206}\text{Pb}/^{208}\text{Pb}$ ratio	\pm (pct)	$^{205}\text{Pb}/^{235}\text{U}$ ratio	\pm (pct)	$^{206}\text{Pb}/^{207}\text{Pb}$ ratio	\pm (pct)	Error correlation	$^{206}\text{Pb}/^{238}\text{U}$ age (m.y.)	\pm (m.y.)	$^{207}\text{Pb}/^{235}\text{U}$ age (m.y.)	\pm (m.y.)	$^{206}\text{Pb}/^{207}\text{Pb}$ age (m.y.)	\pm (m.y.)
48	144	1,684	41	0.01219	5.7	0.09822	7.4	17.11	4.8	0.77	78.1	4.4	95.1	7.3	546	52
49	302	4,056	16	0.01147	0.8	0.07815	4.1	20.23	4.0	0.18	73.5	0.6	76.4	3.2	169	47
50	502	6,319	19	0.01138	0.7	0.07697	2.0	20.39	1.9	0.34	73.0	0.5	75.3	1.6	150	22
51	120	1,781	110	0.01806	4.2	0.14720	7.8	16.91	6.6	0.54	115.4	4.9	139.4	11.7	572	72
52	155	1,032	43	0.01232	2.0	0.08832	5.9	19.23	5.5	0.34	78.9	1.6	85.9	5.3	286	63
53	620	5,940	49	0.01239	0.9	0.08836	1.7	19.34	1.5	0.52	79.4	0.7	86.0	1.6	273	17
54	108	6,800	27	0.05529	2.2	0.40141	2.8	18.99	1.7	0.80	346.9	8.0	342.7	11.4	314	19
55	179	897	40	0.01275	0.8	0.07716	6.8	22.79	6.8	0.12	81.7	0.7	75.5	5.3	-117	83
56	121	1,675	30	0.01206	0.9	0.07180	7.1	23.17	7.1	0.13	77.3	0.7	70.4	5.2	-158	88
57	106	2,235	33	0.01665	1.5	0.11979	6.9	19.17	6.7	0.22	106.5	1.6	114.9	8.3	293	76
58	62	1,056	33	0.01095	2.1	0.05000	16.7	30.20	16.6	0.13	70.2	1.5	49.5	8.5	-865	239
59	295	7,277	28	0.01377	0.8	0.09199	2.2	20.63	2.0	0.39	88.1	0.7	89.4	2.0	122	23
60	728	2,344	79	0.01136	1.0	0.07874	1.9	19.89	1.6	0.54	72.8	0.7	77.0	1.5	208	18
61	113	289	37	0.01589	3.9	0.12301	7.2	17.81	6.1	0.54	101.6	3.9	117.8	8.9	459	67
62	32	829	-9	0.01544	1.0	0.09741	4.6	21.86	4.5	0.21	98.8	0.9	94.4	4.6	-16	55
63	124	1,680	51	0.01203	2.5	0.07329	10.2	22.64	9.9	0.25	77.1	1.9	71.8	7.6	-101	122
64	58	980	144	0.01507	3.0	0.10731	30.7	19.37	30.6	0.10	96.5	2.9	103.5	32.9	269	350
65	178	14,786	23	0.07129	0.9	0.56185	1.2	17.50	0.8	0.76	443.9	4.0	452.7	6.6	498	8
66	201	2,001	22	0.01316	4.2	0.10535	6.1	17.23	4.4	0.69	84.3	3.6	101.7	6.5	532	49
67	113	1,571	116	0.01716	3.1	0.12758	7.7	18.55	7.1	0.40	109.7	3.4	121.9	10.0	368	80
68	128	2,117	34	0.01630	1.6	0.10415	9.9	21.58	9.7	0.16	104.2	1.7	100.6	10.4	15	117
69	65	1,367	72	0.01598	1.3	0.10477	15.7	21.03	15.7	0.08	102.2	1.3	101.2	16.6	77	186
70	340	3,209	38	0.01143	0.7	0.08013	2.7	19.66	2.6	0.27	73.2	0.5	78.3	2.2	234	30

Sample 65

1	351	4,928	454	0.01542	0.5	0.16388	3.8	12.98	3.8	0.12	98.7	0.5	154.1	6.3	1,123	38
2	428	6,085	822	0.01512	0.3	0.10041	3.5	20.77	3.5	0.09	96.8	0.3	97.2	3.5	107	41
3	262	7,204	148	0.01539	0.5	0.10055	3.4	21.11	3.4	0.15	98.5	0.5	97.3	3.5	68	40
4	17	1,514	1,297	0.01092	0.7	0.06172	1.9	24.40	1.7	0.39	70.0	0.5	60.8	1.2	-289	22
5	40	749	131	0.01198	1.0	0.10992	5.8	15.03	5.7	0.17	76.8	0.8	105.9	6.5	823	60
6	60	6,396	51	0.01634	0.6	0.10965	3.0	20.54	2.9	0.19	104.5	0.6	105.6	3.3	133	34
7	15	1,298	91	0.01920	0.9	0.11448	8.1	23.12	8.1	0.11	122.6	1.1	110.1	9.4	-153	100
8	20	2,186	618	0.01563	0.7	0.08967	2.3	24.04	2.2	0.31	100.0	0.7	87.2	2.1	-250	28
9	90	6,466	37	0.01326	0.9	0.09029	8.6	20.25	8.6	0.10	84.9	0.7	87.8	7.9	166	100
10	118	2,122	673	0.01404	0.4	0.08698	2.3	22.25	2.3	0.18	89.9	0.4	84.7	2.0	-59	27
11	94	3,016	65	0.01432	0.4	0.09308	2.1	21.21	2.0	0.20	91.7	0.4	90.4	1.9	56	24
12	23	2,534	811	0.01110	0.5	0.08416	3.4	18.19	3.3	0.16	71.2	0.4	82.0	2.9	411	37
13	101	2,768	43	0.01177	0.5	0.06960	12.4	23.32	12.4	0.04	75.4	0.4	68.3	8.7	-174	155
14	99	4,467	35	0.01509	0.8	0.10817	2.7	19.23	2.5	0.30	96.5	0.8	104.3	2.9	286	29
15	74	3,807	60	0.01191	1.8	0.06255	15.4	26.26	15.3	0.12	76.4	1.4	61.6	9.7	-480	203
0	25	3,560	645	0.01121	1.4	0.07280	7.6	21.24	7.4	0.19	71.9	1.0	71.3	5.6	53	89
17	152	4,936	1,878	0.01138	1.2	0.09541	5.7	16.45	5.5	0.22	73.0	0.9	92.5	5.5	632	59
18	95	3,877	409	0.01227	0.8	0.08354	1.9	20.25	1.7	0.43	78.6	0.6	81.5	1.6	166	20
19	100	3,015	186	0.01773	1.8	0.11738	3.4	20.83	2.9	0.54	113.3	2.1	112.7	4.1	100	34
20	140	3,559	255	0.01233	1.1	0.10911	4.4	15.58	4.2	0.25	79.0	0.9	105.1	4.8	747	45
21	131	6,891	979	0.01334	2.0	0.08362	35.0	21.99	34.9	0.06	85.4	1.7	81.5	29.3	-31	423
22	80	15,088	1,008	0.01158	1.0	0.09213	6.0	17.33	5.9	0.16	74.2	0.7	89.5	5.6	519	65

Table 2. Analytical data on detrital zircons.—Continued

[All analyses by laser-ablation inductively coupled plasma mass spectroscopy (ICPMS)]

Analysis	U content (ppm)	$^{206}\text{Pb}/^{204}\text{Pb}$ ratio	U/Th ratio	$^{206}\text{Pb}/^{208}\text{Pb}$ ratio	\pm (pct)	$^{205}\text{Pb}/^{235}\text{U}$ ratio	\pm (pct)	$^{206}\text{Pb}/^{207}\text{Pb}$ ratio	\pm (pct)	Error correlation	$^{206}\text{Pb}/^{238}\text{U}$ age (m.y.)	\pm (m.y.)	$^{207}\text{Pb}/^{235}\text{U}$ age (m.y.)	\pm (m.y.)	$^{206}\text{Pb}/^{207}\text{Pb}$ age (m.y.)	\pm (m.y.)
23	75	15,568	571	0.02322	0.7	0.16247	3.0	19.70	2.9	0.23	148.0	1.0	152.9	4.9	230	33
24	174	4,918	1,316	0.01420	0.9	0.08991	12.0	21.77	12.0	0.08	90.9	0.8	87.4	10.9	-6	145
25	49	14,056	749	0.01454	0.7	0.09044	4.9	22.16	4.8	0.14	93.0	0.6	87.9	4.5	-49	59
26	64	7,449	283	0.02294	1.0	0.15267	13.2	20.72	13.1	0.07	146.2	1.4	144.3	20.2	113	155
27	491	5,047	819	0.01469	0.6	0.10814	2.3	18.73	2.2	0.25	94.0	0.5	104.3	2.5	346	25
28	173	7,064	599	0.02460	1.1	0.20774	6.6	16.33	6.5	0.16	156.7	1.7	191.7	13.7	648	69
29	86	13,376	538	0.01500	1.0	0.10303	26.6	20.08	26.6	0.04	96.0	0.9	99.6	27.5	186	310
30	195	8,857	2,247	0.01295	1.5	0.10464	16.7	17.07	16.6	0.09	83.0	1.2	101.1	17.6	552	182
31	83	5,270	578	0.02238	1.0	0.14596	7.2	21.14	7.1	0.14	142.7	1.5	138.3	10.6	64	85
32	252	2,185	487	0.01441	0.8	0.08657	28.4	22.95	28.3	0.03	92.2	0.7	84.3	24.6	-135	351
33	86	328,263	323	0.01515	0.4	0.11246	2.5	18.57	2.5	0.16	96.9	0.4	108.2	2.9	365	28
34	134	359,267	2,303	0.01135	0.7	0.07815	5.7	20.02	5.7	0.12	72.7	0.5	76.4	4.5	193	66
35	67	57,499	459	0.02283	1.8	0.21820	7.4	14.43	7.2	0.25	145.5	2.7	200.4	16.2	908	74
36	250	6,817	263	0.01425	0.9	0.09991	4.4	19.66	4.3	0.21	91.2	0.9	96.7	4.5	234	50
37	156	3,704	418	0.01532	0.8	0.10791	25.5	19.57	25.5	0.03	98.0	0.8	104.1	27.6	245	294
38	200	5,147	1,450	0.01122	0.6	0.06267	10.1	24.69	10.1	0.06	71.9	0.4	61.7	6.4	-318	130
39	144	12,849	2,775	0.01846	1.1	0.13672	4.6	18.62	4.4	0.24	117.9	1.3	130.1	6.3	359	50
40	112	6,683	1,007	0.02289	0.5	0.15432	36.8	20.46	36.8	0.01	145.9	0.8	145.7	56.1	142	432
41	189	4,857	319	0.01491	1.3	0.11339	6.2	18.13	6.0	0.21	95.4	1.2	109.1	7.1	419	67
42	144	8,257	867	0.01588	0.7	0.11072	16.8	19.77	16.8	0.04	101.6	0.8	106.6	18.7	221	194
43	84	27,516	523	0.02301	0.6	0.17372	6.4	18.26	6.4	0.10	146.6	0.9	162.6	11.3	402	71
44	80	59,155	477	0.01458	0.5	0.11505	3.0	17.47	2.9	0.18	93.3	0.5	110.6	3.4	501	32
45	95	3,013	1,230	0.01444	0.7	0.09387	64.5	21.21	64.5	0.01	92.4	0.6	91.1	59.7	56	769
46	96	13,330	560	0.01402	0.6	0.09031	89.8	21.41	89.8	0.01	89.8	0.6	87.8	79.2	35	1,076
47	149	84,074	865	0.01441	0.3	0.10482	36.2	18.95	36.2	0.01	92.2	0.3	101.2	37.8	319	411
48	120	5,575	200	0.02786	0.9	0.19307	16.5	19.90	16.5	0.06	177.2	1.6	179.2	31.9	207	191
49	140	7,197	1,113	0.01351	0.5	0.09292	110.1	20.05	110.1	0.00	86.5	0.4	90.2	98.9	189	1,281
50	83	56,074	792	0.01154	0.4	0.08626	1.9	18.44	1.8	0.19	74.0	0.3	84.0	1.6	380	21
51	63	68,167	980	0.01132	0.8	0.08583	3.9	18.18	3.9	0.20	72.6	0.6	83.6	3.4	412	43
52	136	13,640	3,058	0.01550	0.7	0.10353	6.4	20.64	6.4	0.11	99.1	0.7	100.0	6.7	121	75
53	127	9,398	784	0.01475	0.7	0.09983	15.1	20.37	15.1	0.05	94.4	0.7	96.6	15.2	152	177
54	176	10,779	228	0.03180	0.9	0.28310	18.3	15.49	18.3	0.05	201.8	1.9	253.1	51.3	761	193
55	236	13,057	318	0.03206	1.1	0.23295	2.8	18.97	2.6	0.38	203.4	2.2	212.6	6.7	316	30
56	72	37,851	489	0.02344	0.5	0.14014	10.0	23.07	10.0	0.05	149.4	0.8	133.2	14.1	-147	124
57	87	91,888	386	0.01176	0.7	0.08861	6.7	18.30	6.7	0.10	75.4	0.5	86.2	6.0	398	75
58	134	10,571	1,512	0.01451	0.5	0.09262	16.0	21.60	16.0	0.03	92.8	0.5	89.9	14.9	14	192
59	152	3,420	628	0.01225	0.7	0.07430	29.8	22.73	29.8	0.02	78.5	0.6	72.8	22.2	-111	366
60	29	8,657	223	0.02196	1.3	0.16703	6.9	18.13	6.8	0.19	140.1	1.8	156.8	11.7	418	76
61	123	26,665	1,002	0.02195	1.4	0.15348	7.6	19.72	7.5	0.19	139.9	2.0	145.0	11.8	228	87
62	169	7,583	471	0.01080	0.9	0.09186	10.4	16.22	10.3	0.08	69.3	0.6	89.2	9.6	662	111
63	75	35,515	847	0.01650	1.1	0.10980	9.8	20.72	9.7	0.11	105.5	1.2	105.8	10.8	112	115
64	54	6,482	418	0.01147	0.6	0.07191	18.7	22.00	18.6	0.03	73.5	0.5	70.5	13.5	-31	226
65	84	30,396	222	0.02982	0.7	0.21322	1.6	19.28	1.4	0.44	189.4	1.3	196.3	3.4	279	16
66	116	7,549	85	0.22531	1.2	2.76964	10.1	11.22	10.0	0.12	1,309.9	17.4	1,347.4	250.1	1,407	96
67	75	17,178	940	0.01452	0.3	0.10509	5.0	19.05	5.0	0.06	92.9	0.3	101.5	5.3	308	57
68	159	14,525	2,852	0.01267	0.5	0.09377	8.6	18.63	8.6	0.05	81.2	0.4	91.0	8.2	358	97
69	79	38,454	438	0.01176	1.4	0.09035	10.6	17.94	10.5	0.13	75.4	1.1	87.8	9.7	442	117
70	162	6,862	1,664	0.01099	1.1	0.08471	18.5	17.90	18.4	0.06	70.5	0.8	82.6	15.8	448	205

Table 2. Analytical data on detrital zircons.—Continued

[All analyses by laser-ablation inductively coupled plasma mass spectroscopy (ICPMS)]

Analysis	U content (ppm)	$^{206}\text{Pb}/^{204}\text{Pb}$ ratio	U/Th ratio	$^{206}\text{Pb}/^{208}\text{Pb}$ ratio	\pm (pct)	$^{205}\text{Pb}/^{235}\text{U}$ ratio	\pm (pct)	$^{206}\text{Pb}/^{207}\text{Pb}$ ratio	\pm (pct)	Error correlation	$^{206}\text{Pb}/^{238}\text{U}$ age (m.y.)	\pm (m.y.)	$^{207}\text{Pb}/^{235}\text{U}$ age (m.y.)	\pm (m.y.)	$^{206}\text{Pb}/^{207}\text{Pb}$ age (m.y.)	\pm (m.y.)
<i>Sample 66</i>																
1	136	1,409	33	0.03093	1.6	0.19120	5.4	22.31	5.2	0.29	196.4	3.1	177.7	10.4	-65	63
2	49	1,124	38	0.01673	1.5	0.08353	34.7	27.62	34.7	0.04	107.0	1.6	81.5	29.0	-615	473
3	57	1,371	24	0.02531	0.9	0.17375	11.2	20.09	11.1	0.08	161.2	1.5	162.7	19.5	185	129
4	124	1,621	58	0.01765	36.2	0.11735	39.0	20.74	14.4	0.93	112.8	41.1	112.7	45.4	110	170
5	43	838	26	0.02652	1.7	0.19644	22.4	18.62	22.4	0.07	168.8	2.9	182.1	43.8	359	252
6	68	571	19	0.01961	1.4	0.15948	13.6	16.96	13.5	0.10	125.2	1.7	150.2	21.7	566	147
7	176	3,182	22	0.02363	2.3	0.15470	4.0	21.06	3.3	0.57	150.5	3.5	146.1	6.3	74	39
8	102	2,019	24	0.02484	2.2	0.16502	8.7	20.75	8.4	0.25	158.2	3.5	155.1	14.5	108	99
9	97	1,765	30	0.01687	1.0	0.10689	13.4	21.76	13.3	0.08	107.8	1.1	103.1	14.4	-5	161
10	309	2,455	20	0.01627	1.5	0.11017	4.2	20.36	3.9	0.35	104.1	1.5	106.1	4.7	153	46
11	67	1,057	23	0.01970	2.5	0.11622	9.1	23.37	8.8	0.28	125.7	3.2	111.6	10.7	-180	109
12	72	1,088	57	0.01660	2.8	0.09292	9.9	24.63	9.5	0.29	106.1	3.0	90.2	9.3	-313	121
13	67	1,142	66	0.02296	3.2	0.13832	8.7	22.89	8.1	0.37	146.3	4.7	131.5	12.1	-128	100
14	191	1,602	19	0.01609	1.6	0.10667	4.0	20.80	3.7	0.39	102.9	1.6	102.9	4.3	103	44
15	84	1,304	32	0.01717	1.9	0.10284	10.0	23.02	9.8	0.19	109.7	2.1	99.4	10.4	-142	121
16	200	1,651	20	0.01618	2.2	0.10037	4.3	22.23	3.7	0.50	103.5	2.3	97.1	4.4	-57	45
17	55	1,226	17	0.02506	1.1	0.13134	11.5	26.31	11.5	0.10	159.6	1.8	125.3	15.3	-485	152
18	199	2,367	25	0.01629	1.8	0.10275	4.1	21.86	3.7	0.44	104.2	1.9	99.3	4.3	-15	45
19	135	2,082	32	0.01660	0.9	0.11173	6.7	20.49	6.6	0.14	106.1	1.0	107.6	7.6	139	78
20	83	2,412	22	0.01802	2.2	0.13285	14.8	18.71	14.6	0.15	115.2	2.5	126.7	19.8	348	165
21	87	2,277	32	0.02389	2.2	0.17692	11.1	18.62	10.9	0.20	152.2	3.4	165.4	19.8	359	123
22	82	1,378	27	0.02507	2.0	0.16606	10.2	20.81	10.0	0.19	159.6	3.1	156.0	17.0	102	118
23	74	2,119	19	0.02667	1.6	0.22040	9.6	16.69	9.5	0.17	169.7	2.8	202.2	21.3	601	103
24	118	5,593	21	0.05711	1.4	0.42880	2.5	18.36	2.1	0.57	358.0	5.2	362.3	10.8	390	23
25	108	1,542	22	0.01939	1.2	0.14609	10.2	18.30	10.1	0.12	123.8	1.5	138.5	15.0	398	113
26	62	1,229	19	0.02405	1.9	0.15134	10.4	21.92	10.2	0.19	153.2	3.0	143.1	15.8	-22	123
27	105	1,818	20	0.01638	1.7	0.08838	16.4	25.56	16.3	0.11	104.7	1.8	86.0	14.6	-408	213
28	53	1,574	25	0.02400	1.1	0.16165	12.4	20.47	12.4	0.09	152.9	1.7	152.1	20.2	141	145
29	41	1,277	21	0.02514	1.1	0.12795	8.9	27.09	8.8	0.12	160.1	1.8	122.3	11.4	-563	118
30	77	1,569	40	0.02551	1.7	0.16608	6.1	21.18	5.8	0.28	162.4	2.8	156.0	10.2	60	69
31	181	943	19	0.01578	2.0	0.09816	9.1	22.16	8.8	0.23	100.9	2.1	95.1	9.0	-49	107
32	124	1,511	26	0.01618	1.2	0.11573	7.4	19.27	7.3	0.17	103.4	1.3	111.2	8.6	281	83
33	157	2,551	18	0.01652	1.5	0.10246	6.7	22.23	6.5	0.22	105.6	1.6	99.0	6.9	-56	80
34	87	1,780	31	0.01806	2.6	0.11037	14.2	22.56	13.9	0.19	115.4	3.1	106.3	15.8	-93	171
35	57	1,352	15	0.02418	1.6	0.14425	15.7	23.11	15.6	0.10	154.0	2.5	136.8	22.8	-152	194
36	35	2,015	30	0.02549	2.1	0.15932	25.5	22.06	25.4	0.08	162.3	3.5	150.1	40.4	-38	308
37	156	4,133	28	0.02444	1.6	0.15304	5.2	22.02	5.0	0.31	155.7	2.6	144.6	8.1	-34	60
38	67	3,413	18	0.02427	1.2	0.15077	10.1	22.19	10.0	0.12	154.6	1.8	142.6	15.3	-52	122
39	692	18,764	14	0.03556	2.3	0.27225	2.6	18.01	1.3	0.87	225.3	5.2	244.5	7.2	433	14
40	73	2,193	22	0.03373	4.2	0.19837	9.5	23.45	8.5	0.44	213.9	9.1	183.7	18.9	-188	106
41	95	1,589	62	0.03730	5.1	0.30566	13.0	16.83	12.0	0.39	236.1	12.2	270.8	39.5	583	130
42	71	1,869	24	0.02470	1.8	0.12768	13.5	26.67	13.4	0.13	157.3	2.8	122.0	17.4	-521	179
43	39	1,109	33	0.02519	1.8	0.15179	16.3	22.88	16.2	0.11	160.4	3.0	143.5	24.9	-127	200
44	57	1,392	16	0.02364	1.8	0.13432	12.7	24.27	12.6	0.14	150.6	2.7	128.0	17.1	-275	160
45	80	1,886	23	0.01693	1.5	0.11483	9.2	20.33	9.1	0.16	108.2	1.6	110.4	10.6	157	106
46	59	1,023	30	0.01930	2.8	0.13833	13.0	19.23	12.7	0.22	123.2	3.5	131.6	18.0	285	145

Table 2. Analytical data on detrital zircons.—Continued

[All analyses by laser-ablation inductively coupled plasma mass spectroscopy (ICPMS)]

Analysis	U content (ppm)	$^{206}\text{Pb}/^{204}\text{Pb}$ ratio	U/Th ratio	$^{206}\text{Pb}/^{208}\text{Pb}$ ratio	± (pct)	$^{205}\text{Pb}/^{235}\text{U}$ ratio	± (pct)	$^{206}\text{Pb}/^{207}\text{Pb}$ ratio	± (pct)	Error correlation	$^{206}\text{Pb}/^{238}\text{U}$ age (m.y.)	± (m.y.)	$^{207}\text{Pb}/^{235}\text{U}$ age (m.y.)	± (m.y.)	$^{206}\text{Pb}/^{207}\text{Pb}$ age (m.y.)	± (m.y.)
47	89	646	51	0.02134	1.5	0.16572	6.8	17.76	6.6	0.22	136.1	2.0	155.7	11.3	465	73
48	68	1,578	32	0.02341	1.7	0.14529	4.8	22.21	4.5	0.35	149.2	2.5	137.7	7.1	-55	55
49	83	2,033	75	0.01885	2.3	0.10998	16.2	23.64	16.1	0.14	120.4	2.8	105.9	18.0	-208	202
50	104	3,325	42	0.02513	1.1	0.16130	6.3	21.48	6.2	0.18	160.0	1.8	151.8	10.2	26	74
51	78	1,201	32	0.02468	1.0	0.18417	7.5	18.48	7.4	0.13	157.2	1.5	171.6	13.9	376	83
52	62	1,838	22	0.02624	2.4	0.20637	10.6	17.53	10.4	0.22	167.0	4.0	190.5	22.0	493	114
53	161	2,911	21	0.02518	2.0	0.16737	4.5	20.74	4.0	0.44	160.3	3.2	157.1	7.6	109	48
54	108	1,742	56	0.01740	2.7	0.11020	8.0	21.77	7.5	0.34	111.2	3.1	106.1	8.9	-5	90
55	97	1,993	24	0.01630	1.7	0.10475	6.4	21.46	6.1	0.27	104.3	1.8	101.2	6.7	29	73
56	111	2,437	23	0.01608	2.5	0.11789	12.1	18.81	11.9	0.21	102.9	2.6	113.2	14.4	336	134
57	90	1,562	63	0.01706	2.1	0.13934	12.6	16.88	12.4	0.17	109.1	2.3	132.5	17.7	576	135
58	37	301	33	0.01702	3.5	0.08843	20.8	26.54	20.5	0.17	108.8	3.8	86.0	18.5	-508	274
59	47	1,181	33	0.02343	1.3	0.13513	12.0	23.90	11.9	0.11	149.3	2.0	128.7	16.3	-236	150
60	670	10,910	12	0.01594	1.5	0.10848	2.6	20.27	2.2	0.56	102.0	1.5	104.6	2.9	164	25
61	72	846	35	0.01640	1.7	0.10256	18.9	22.05	18.8	0.09	104.9	1.7	99.1	19.5	-37	229
62	57	1,547	43	0.02472	2.8	0.18774	13.9	18.16	13.6	0.20	157.4	4.5	174.7	26.1	415	152
63	57	3,359	55	0.05664	4.2	0.43978	6.2	17.76	4.6	0.68	355.2	15.2	370.1	27.2	465	50
64	144	2,468	33	0.01649	1.9	0.12716	7.5	17.88	7.3	0.25	105.5	2.0	121.5	9.7	449	81
65	51	1,631	120	0.02400	5.6	0.15258	6.3	21.69	3.0	0.88	152.9	8.6	144.2	9.8	3	37
66	60	1,327	30	0.02368	3.4	0.13297	15.8	24.56	15.4	0.22	150.9	5.2	126.8	21.0	-305	197
67	73	1,711	29	0.02584	1.2	0.21168	13.7	16.83	13.6	0.09	164.5	2.0	195.0	29.0	582	148
68	88	1,397	23	0.01622	2.3	0.10255	15.5	21.81	15.3	0.15	103.7	2.4	99.1	16.0	-10	185
69	67	925	57	0.01816	1.4	0.11657	28.0	21.49	28.0	0.05	116.0	1.6	112.0	32.6	26	335
70	60	1,405	42	0.01491	3.5	0.09236	48.0	22.26	47.9	0.07	95.4	3.4	89.7	44.0	-59	583

Sample 67

1	351	9,857	332	0.01581	0.9	0.09892	2.2	22.04	1.9	0.43	101.1	0.9	95.8	2.2	-35	24
2	428	12,170	413	0.02329	0.8	0.22182	3.6	14.48	3.5	0.23	148.4	1.2	203.4	8.1	901	36
3	262	14,409	69	0.02645	0.3	0.23517	6.2	15.51	6.2	0.05	168.3	0.6	214.5	14.7	757	65
4	17	3,028	696	0.01675	0.9	0.09069	9.9	25.47	9.8	0.09	107.1	0.9	88.1	9.0	-399	128
5	40	1,499	60	0.02261	1.3	0.12452	14.5	25.03	14.5	0.09	144.1	1.9	119.2	18.2	-354	187
6	60	1,279	47	0.01658	1.4	0.07857	30.7	29.10	30.7	0.05	106.0	1.5	76.8	24.2	-760	431
7	15	2,597	46	0.03599	1.5	0.25001	10.4	19.85	10.3	0.15	227.9	3.6	226.6	26.0	213	119
8	20	4,372	351	0.02615	0.8	0.16989	4.5	21.22	4.4	0.18	166.4	1.4	159.3	7.7	55	53
9	90	12,933	26	0.01808	0.7	0.12414	4.7	20.08	4.7	0.14	115.5	0.8	118.8	5.9	186	54
10	118	4,243	527	0.01697	1.0	0.09861	7.6	23.73	7.5	0.14	108.5	1.1	95.5	7.5	-218	94
11	94	6,032	33	0.02677	0.8	0.18569	3.3	19.88	3.2	0.23	170.3	1.3	172.9	6.2	209	37
12	23	5,068	361	0.02373	1.2	0.15052	3.4	21.74	3.1	0.36	151.2	1.9	142.4	5.1	-2	38
13	101	5,537	19	0.02451	1.1	0.16819	5.8	20.09	5.7	0.18	156.1	1.7	157.8	9.9	185	67
14	99	8,935	30	0.01683	0.5	0.11587	2.4	20.03	2.3	0.22	107.6	0.6	111.3	2.8	192	27
15	74	7,615	44	0.01640	1.0	0.09205	21.3	23.25	21.3	0.05	99.3	1.0	89.4	19.7	-166	265
16	25	7,121	420	0.01552	1.1	0.09951	12.7	22.73	12.7	0.09	104.9	1.1	96.3	12.8	-110	156
17	152	9,871	1,178	0.01731	0.6	0.16349	2.2	14.60	2.2	0.26	110.6	0.7	153.8	3.7	884	22
18	95	7,753	140	0.03429	0.7	0.23412	1.3	20.19	1.1	0.53	217.3	1.5	213.6	3.1	173	13
19	100	6,031	199	0.01585	1.0	0.09940	21.8	21.98	21.8	0.05	101.4	1.0	96.2	21.8	-29	264
20	140	712	181	0.01661	2.0	0.07504	69.0	30.51	68.9	0.03	106.2	2.1	73.5	51.2	-895	999
21	131	13,782	524	0.02388	0.6	0.16830	1.9	19.57	1.8	0.30	152.2	0.9	157.9	3.3	246	21

Table 2. Analytical data on detrital zircons.—Continued

[All analyses by laser-ablation inductively coupled plasma mass spectroscopy (ICPMS)]

Analysis	U content (ppm)	$^{206}\text{Pb}/^{204}\text{Pb}$ ratio	U/Th ratio	$^{206}\text{Pb}/^{208}\text{Pb}$ ratio	\pm (pct)	$^{205}\text{Pb}/^{235}\text{U}$ ratio	\pm (pct)	$^{206}\text{Pb}/^{207}\text{Pb}$ ratio	\pm (pct)	Error correlation	$^{206}\text{Pb}/^{238}\text{U}$ age (m.y.)	\pm (m.y.)	$^{207}\text{Pb}/^{235}\text{U}$ age (m.y.)	\pm (m.y.)	$^{206}\text{Pb}/^{207}\text{Pb}$ age (m.y.)	\pm (m.y.)
22	80	30,177	310	0.03622	0.8	0.27452	1.5	18.19	1.3	0.52	229.4	1.9	246.3	4.3	411	15
23	75	31,137	761	0.01661	0.5	0.12607	4.9	18.17	4.9	0.09	106.2	0.5	120.6	6.3	414	55
24	174	9,836	1,071	0.01671	0.7	0.10260	18.1	22.46	18.1	0.04	106.8	0.7	99.2	18.7	-81	221
25	49	14,056	613	0.01702	1.0	0.11321	10.3	20.73	10.2	0.10	108.8	1.1	108.9	11.8	111	121
26	64	7,449	353	0.01757	0.8	0.10713	35.3	22.61	35.3	0.02	112.3	0.9	103.3	37.7	-98	434
27	491	5,047	699	0.01651	0.7	0.10751	4.2	21.18	4.1	0.17	105.6	0.7	103.7	4.5	61	49
28	173	7,064	874	0.01613	0.8	0.10658	3.7	20.87	3.6	0.22	103.2	0.9	102.8	4.0	95	43
29	86	13,376	473	0.01640	1.6	0.13475	6.1	16.78	5.9	0.26	104.9	1.7	128.4	8.4	589	64
30	195	8,857	1,709	0.01638	0.9	0.11190	13.8	20.18	13.7	0.06	104.7	0.9	107.7	15.5	174	160
31	83	5,270	772	0.01608	0.8	0.09930	6.6	22.33	6.6	0.12	102.8	0.8	96.1	6.6	-67	80
32	252	2,185	276	0.02455	1.5	0.14990	55.8	22.58	55.8	0.03	156.4	2.4	141.8	81.6	-95	685
33	86	328,263	273	0.01727	0.6	0.12217	6.4	19.49	6.3	0.10	110.4	0.7	117.0	7.8	255	73
34	134	359,267	1,017	0.02486	0.7	0.18770	4.8	18.26	4.8	0.14	158.3	1.1	174.7	9.1	402	53
35	67	57,499	642	0.01571	0.8	0.11247	3.8	19.26	3.7	0.20	100.5	0.8	108.2	4.3	283	43
36	250	6,817	141	0.02578	1.0	0.17314	19.1	20.53	19.0	0.05	164.1	1.6	162.1	33.0	134	224
37	156	3,704	375	0.01649	0.3	0.11106	4.8	20.48	4.8	0.06	105.5	0.3	106.9	5.4	140	56
38	200	5,147	600	0.02637	1.3	0.18161	32.3	20.02	32.3	0.04	167.8	2.2	169.4	57.8	193	375
39	144	12,849	2,884	0.01717	0.8	0.12969	6.4	18.26	6.3	0.12	109.7	0.9	123.8	8.3	403	71
40	112	6,683	1,391	0.01599	0.4	0.11096	13.1	19.87	13.1	0.03	102.3	0.4	106.8	14.6	210	152
41	189	4,857	289	0.01596	0.5	0.10463	27.6	21.03	27.6	0.02	102.0	0.5	101.0	28.9	78	327
42	144	8,257	829	0.01610	0.5	0.14396	4.6	15.42	4.6	0.11	102.9	0.5	136.6	6.7	770	48
43	84	27,516	717	0.01624	0.6	0.11178	5.0	20.03	4.9	0.11	103.8	0.6	107.6	5.6	191	57
44	80	59,155	270	0.02505	1.5	0.19207	2.3	17.99	1.7	0.65	159.5	2.4	178.4	4.5	436	19
45	95	3,013	496	0.03504	0.8	0.22701	38.0	21.28	38.0	0.02	222.0	1.8	207.7	84.0	48	454
47	149	3,109	395	0.03086	1.7	0.18757	4.2	22.69	3.9	0.41	196.0	3.4	174.6	8.0	-106	47
48	120	5,575	325	0.01664	0.7	0.15150	5.0	15.15	5.0	0.15	106.4	0.8	143.2	7.7	807	52
49	140	7,197	930	0.01576	1.0	0.10425	4.9	20.84	4.8	0.20	100.8	1.0	100.7	5.2	98	57
50	83	56,074	579	0.01541	0.8	0.13274	8.4	16.00	8.3	0.10	98.6	0.8	126.6	11.2	691	89
51	63	68,167	589	0.01842	1.8	0.15256	6.0	16.65	5.7	0.30	117.7	2.1	144.2	9.2	606	61
52	136	13,640	1,307	0.03566	1.0	0.24874	5.4	19.77	5.3	0.19	225.9	2.3	225.6	13.4	222	61
53	127	9,398	450	0.02522	0.7	0.17441	16.3	19.94	16.3	0.04	160.6	1.1	163.2	28.5	202	189
54	176	10,779	433	0.01634	0.8	0.12017	3.0	18.75	2.9	0.27	104.5	0.9	115.2	3.7	343	33
55	236	13,057	598	0.01659	0.9	0.11286	9.8	20.27	9.7	0.10	106.1	1.0	108.6	11.1	164	114
56	72	37,851	651	0.01722	0.4	0.11072	2.7	21.44	2.7	0.14	110.0	0.4	106.6	3.1	31	32
57	87	91,888	281	0.01582	0.6	0.10011	5.7	21.80	5.6	0.10	101.2	0.6	96.9	5.7	-9	68
58	134	10,571	1,342	0.01604	0.7	0.11428	5.1	19.35	5.0	0.14	102.6	0.7	109.9	5.9	271	57
59	152	3,420	313	0.02427	0.7	0.17284	5.3	19.36	5.2	0.14	154.6	1.1	161.9	9.2	270	60
60	29	8,657	296	0.01627	0.7	0.09600	6.3	23.36	6.3	0.10	104.0	0.7	93.1	6.2	-179	79
61	123	26,665	885	0.02446	0.6	0.16215	3.0	20.80	2.9	0.19	155.8	0.9	152.6	4.9	103	34
62	169	7,583	302	0.01661	0.4	0.11163	2.5	20.51	2.4	0.18	106.2	0.5	107.5	2.8	136	29
63	75	35,515	559	0.02469	0.5	0.16793	0.7	20.27	0.5	0.69	157.2	0.8	157.6	1.3	163	6
64	54	6,482	195	0.02436	0.9	0.16369	5.3	20.52	5.3	0.16	155.2	1.3	153.9	8.8	135	62
65	84	30,396	400	0.01623	0.7	0.10086	8.0	22.18	8.0	0.09	103.8	0.7	97.6	8.2	-52	97
66	116	7,549	1,033	0.01718	0.7	0.11840	2.2	20.00	2.1	0.33	109.8	0.8	113.6	2.7	195	24
67	75	17,178	840	0.01607	0.4	0.11113	3.3	19.93	3.3	0.11	102.7	0.4	107.0	3.7	203	38
68	159	14,525	2,129	0.01680	0.5	0.11023	2.8	21.02	2.8	0.16	107.4	0.5	106.2	3.2	79	33
69	79	38,454	208	0.02458	1.0	0.17568	4.2	19.29	4.1	0.24	156.6	1.6	164.3	7.4	278	46
70	162	6,862	1,124	0.01613	0.5	0.10965	7.4	20.29	7.4	0.07	103.2	0.5	105.6	8.2	162	86
71	351	4,928	340	0.01622	0.6	0.09962	25.9	22.45	25.9	0.02	103.7	0.6	96.4	25.9	-80	317
72	428	6,085	588	0.01721	1.2	0.16509	7.4	14.38	7.3	0.16	110.0	1.3	155.1	12.3	915	75

Table 2. Analytical data on detrital zircons.—Continued

[All analyses by laser-ablation inductively coupled plasma mass spectroscopy (ICPMS)]

Analysis	U content (ppm)	$^{206}\text{Pb}/^{204}\text{Pb}$ ratio	U/Th ratio	$^{206}\text{Pb}/^{208}\text{Pb}$ ratio	\pm (pct)	$^{205}\text{Pb}/^{235}\text{U}$ ratio	\pm (pct)	$^{206}\text{Pb}/^{207}\text{Pb}$ ratio	\pm (pct)	Error correlation	$^{206}\text{Pb}/^{238}\text{U}$ age (m.y.)	\pm (m.y.)	$^{207}\text{Pb}/^{235}\text{U}$ age (m.y.)	\pm (m.y.)	$^{206}\text{Pb}/^{207}\text{Pb}$ age (m.y.)	\pm (m.y.)
73	262	7,204	79	0.02433	0.7	0.15004	3.7	22.36	3.7	0.18	155.0	1.0	142.0	5.6	-70	45
74	17	4,542	515	0.02390	0.5	0.15570	4.5	21.17	4.4	0.12	152.3	0.8	146.9	7.0	62	53
75	40	2,248	65	0.02192	0.7	0.14052	24.4	21.51	24.4	0.03	139.8	1.0	133.5	34.3	23	293
<i>Sample 69</i>																
1	25	842	40	0.02287	0.9	0.10330	26.1	30.52	26.1	0.03	145.7	1.3	99.8	27.0	-896	378
2	45	1,015	43	0.01553	1.3	0.07209	32.3	29.70	32.3	0.04	99.3	1.3	70.7	23.4	-817	460
3	103	1,379	33	0.01518	0.9	0.07907	7.5	26.47	7.5	0.13	97.1	0.9	77.3	6.0	-501	99
4	53	3,941	61	0.06115	0.8	0.43786	3.6	19.26	3.5	0.22	382.6	3.2	368.7	16.0	282	40
5	81	1,903	64	0.02382	0.8	0.13803	4.5	23.80	4.4	0.18	151.8	1.2	131.3	6.3	-225	56
6	179	2,316	47	0.01400	1.2	0.08890	4.9	21.71	4.8	0.24	89.6	1.1	86.5	4.4	1	58
7	201	5,794	43	0.02591	1.0	0.17838	2.3	20.03	2.1	0.43	164.9	1.6	166.7	4.2	192	24
8	100	4,728	42	0.04168	1.0	0.27805	2.9	20.67	2.7	0.34	263.2	2.6	249.1	8.0	118	32
9	47	1,924	57	0.01835	2.9	0.10152	38.6	24.92	38.5	0.07	117.2	3.4	98.2	39.0	-342	496
10	59	1,659	20	0.02317	1.2	0.13700	10.1	23.32	10.0	0.12	147.7	1.8	130.4	13.9	-174	125
11	73	1,770	55	0.02781	3.9	0.17364	12.8	22.08	12.2	0.30	176.8	7.0	162.6	22.3	-40	148
12	61	2,065	59	0.02236	0.8	0.12505	12.6	24.66	12.5	0.06	142.6	1.1	119.6	15.8	-316	161
13	89	4,392	19	0.02252	0.9	0.14038	10.7	22.12	10.7	0.09	143.6	1.3	133.4	15.1	-45	129
14	71	677	36	0.01614	1.9	0.09680	11.7	22.99	11.5	0.17	103.2	2.0	93.8	11.4	-139	143
15	37	1,265	25	0.02261	1.3	0.13465	12.0	23.15	11.9	0.11	144.1	1.9	128.3	16.3	-156	148
16	119	2,020	53	0.01362	0.7	0.07704	4.5	24.37	4.5	0.16	87.2	0.6	75.4	3.5	-285	57
17	249	5,577	35	0.01468	0.5	0.09890	4.5	20.46	4.5	0.10	93.9	0.4	95.8	4.5	142	53
18	137	2,654	20	0.01422	0.7	0.08627	5.4	22.73	5.3	0.13	91.1	0.6	84.0	4.7	-111	65
19	66	3,275	24	0.02275	1.2	0.11896	12.9	26.36	12.9	0.09	145.0	1.7	114.1	15.5	-490	171
20	200	6,985	25	0.01496	0.8	0.09813	4.9	21.02	4.8	0.17	95.7	0.8	95.0	4.8	78	57
21	40	1,358	31	0.02152	1.6	0.11897	21.0	24.95	20.9	0.07	137.3	2.2	114.1	25.0	-345	270
22	22	561	250	0.02662	2.6	0.26297	31.4	13.96	31.2	0.08	169.4	4.5	237.1	80.4	976	318
23	43	1,243	18	0.02280	1.4	0.12379	12.9	25.39	12.8	0.11	145.3	2.0	118.5	16.0	-391	166
24	104	4,837	65	0.01529	1.1	0.11228	11.1	18.78	11.1	0.09	97.8	1.0	108.0	12.6	339	125
25	63	996	76	0.01696	3.3	0.11500	16.3	20.34	15.9	0.21	108.4	3.6	110.5	18.8	156	186
26	132	6,975	29	0.01511	1.1	0.09885	7.9	21.07	7.8	0.14	96.7	1.1	95.7	7.9	72	93
27	73	2,150	26	0.02288	1.4	0.14034	6.2	22.48	6.0	0.23	145.8	2.1	133.3	8.8	-84	74
28	74	3,609	17	0.02071	0.9	0.14631	3.9	19.51	3.8	0.23	132.1	1.2	138.7	5.8	252	44
29	68	1,088	24	0.01433	1.0	0.07724	15.8	25.58	15.8	0.06	91.7	0.9	75.5	12.3	-410	206
30	48	1,170	21	0.02267	1.0	0.10972	9.7	28.48	9.7	0.10	144.5	1.4	105.7	10.8	-700	134
31	41	648	68	0.01462	1.6	0.05866	16.9	34.36	16.9	0.09	93.5	1.5	57.9	10.0	-1253	265
32	1,341	45,289	10	0.03200	1.0	0.23019	1.2	19.17	0.6	0.87	203.1	2.1	210.4	2.8	293	7
33	242	3,240	52	0.01526	1.4	0.08797	4.4	23.92	4.1	0.32	97.6	1.4	85.6	3.9	-239	52
34	114	2,683	23	0.01494	0.9	0.09948	8.7	20.70	8.7	0.10	95.6	0.8	96.3	8.8	114	103
35	61	1,836	38	0.02312	2.5	0.11138	9.5	28.62	9.1	0.27	147.3	3.8	107.2	10.7	-713	127
36	120	4,992	26	0.03340	0.8	0.21836	2.6	21.09	2.5	0.31	211.8	1.8	200.5	5.8	70	30
37	173	3,576	19	0.01559	0.9	0.09863	4.2	21.80	4.1	0.20	99.8	0.8	95.5	4.2	-9	50
38	124	2,362	29	0.01629	2.3	0.09755	5.4	23.03	4.8	0.43	104.2	2.4	94.5	5.3	-143	60
39	65	1,851	21	0.02442	2.0	0.14806	8.7	22.74	8.5	0.23	155.5	3.2	140.2	13.0	-112	105
40	60	1,462	46	0.02416	3.0	0.15412	10.8	21.61	10.4	0.28	153.9	4.6	145.5	16.7	12	124
41	134	4,246	15	0.02381	0.9	0.15401	4.2	21.32	4.1	0.22	151.7	1.4	145.5	6.5	44	48
42	70	1,949	35	0.02641	2.2	0.17493	8.9	20.81	8.6	0.25	168.0	3.7	163.7	15.7	102	102

Table 2. Analytical data on detrital zircons.

[All analyses by laser-ablation inductively coupled plasma mass spectroscopy (ICPMS)]

Analysis	U content (ppm)	$^{206}\text{Pb}/^{204}\text{Pb}$ ratio	U/Th ratio	$^{206}\text{Pb}/^{208}\text{Pb}$ ratio	\pm (pct)	$^{205}\text{Pb}/^{235}\text{U}$ ratio	\pm (pct)	$^{206}\text{Pb}/^{207}\text{Pb}$ ratio	\pm (pct)	Error correlation	$^{206}\text{Pb}/^{238}\text{U}$ age (m.y.)	\pm (m.y.)	$^{207}\text{Pb}/^{235}\text{U}$ age (m.y.)	\pm (m.y.)	$^{206}\text{Pb}/^{207}\text{Pb}$ age (m.y.)	\pm (m.y.)
43	68	2,025	28	0.02839	3.2	0.16739	8.3	23.39	7.7	0.38	180.5	5.8	157.1	14.0	-182	96
44	137	3,031	22	0.02255	0.9	0.14658	3.6	21.22	3.4	0.25	143.8	1.3	138.9	5.3	56	41
45	79	2,484	54	0.03677	0.5	0.24964	6.3	20.31	6.2	0.08	232.8	1.1	226.3	15.7	159	73
46	112	2,152	24	0.02173	0.6	0.13592	7.4	22.04	7.4	0.08	138.6	0.9	129.4	10.2	-36	90
47	83	2,526	44	0.02592	1.0	0.17981	3.5	19.88	3.4	0.28	165.0	1.7	167.9	6.4	209	39
48	305	6,703	14	0.02118	1.3	0.14224	2.7	20.53	2.3	0.49	135.1	1.8	135.0	3.9	134	28
49	229	5,653	40	0.03472	0.6	0.25251	1.8	18.96	1.7	0.35	220.0	1.4	228.6	4.6	318	19
50	133	3,874	73	0.02510	2.6	0.17077	5.2	20.27	4.5	0.50	159.8	4.2	160.1	9.0	164	53
51	267	3,995	52	0.01966	3.7	0.13103	5.0	20.69	3.4	0.74	125.5	4.7	125.0	6.6	115	40
52	68	1,714	79	0.02576	1.5	0.19141	8.3	18.56	8.2	0.18	164.0	2.5	177.8	16.0	367	92
53	471	5,846	47	0.01612	1.5	0.10415	1.9	21.34	1.3	0.76	103.1	1.5	100.6	2.0	43	15
54	137	2,823	71	0.01984	2.0	0.13186	5.2	20.75	4.8	0.38	126.7	2.5	125.8	6.9	109	57
55	179	4,260	38	0.02394	1.4	0.15326	4.5	21.53	4.3	0.30	152.5	2.1	144.8	7.0	21	52
56	295	6,890	22	0.02318	0.8	0.15826	2.0	20.20	1.9	0.39	147.7	1.2	149.2	3.2	172	22
57	69	2,487	25	0.02776	2.6	0.19558	8.2	19.57	7.8	0.32	176.5	4.6	181.4	16.2	245	90
58	69	1,265	30	0.02553	2.2	0.13430	4.6	26.21	4.1	0.46	162.5	3.5	128.0	6.3	-474	54
59	105	3,750	53	0.02343	1.9	0.16386	4.8	19.71	4.4	0.39	149.3	2.8	154.1	7.9	228	51
60	194	5,028	14	0.03107	0.9	0.21431	2.0	19.99	1.8	0.46	197.3	1.8	197.2	4.3	196	21
61	77	1,922	31	0.02295	1.6	0.14263	5.8	22.19	5.6	0.28	146.3	2.4	135.4	8.4	-52	68
62	745	5,856	43	0.02696	1.5	0.18534	2.2	20.06	1.6	0.68	171.5	2.6	172.6	4.1	188	19
63	106	1,852	101	0.02113	2.6	0.13920	14.1	20.93	13.8	0.19	134.8	3.6	132.3	19.7	88	164
64	90	955	70	0.02381	1.3	0.14263	5.6	23.01	5.5	0.22	151.7	1.9	135.4	8.1	-142	68
65	198	2,938	55	0.01595	1.5	0.10277	4.2	21.40	3.9	0.36	102.0	1.6	99.3	4.4	35	47
66	77	1,443	61	0.02278	1.0	0.11866	10.6	26.46	10.5	0.09	145.2	1.5	113.9	12.7	-500	140
67	67	1,261	56	0.02467	4.5	0.15255	9.5	22.30	8.4	0.47	157.1	7.2	144.2	14.6	-64	102
68	86	1,120	28	0.01566	1.4	0.08348	9.0	25.86	8.9	0.15	100.1	1.4	81.4	7.6	-439	117
69	163	2,549	21	0.02237	0.9	0.16881	6.4	18.28	6.3	0.14	142.6	1.3	158.4	10.9	401	71
70	135	2,362	28	0.01571	0.7	0.11183	7.7	19.37	7.7	0.09	100.5	0.7	107.6	8.7	269	88